NANO · MICRO small
www.small-journal.com

# Smart Film Actuators for Biomedical Applications

*Zhuohao Zhang, Yu Wang, Qiao Wang, and Luoran Shang**

**Taking inspiration from the extremely flexible motion abilities in natural organisms, soft actuators have emerged in the past few decades. Particularly, smart film actuators (SFAs) demonstrate unique superiority in easy fabrication, tailorable geometric configurations, and programmable 3D deformations. Thus, they are promising in many biomedical applications, such as soft robotics, tissue engineering, delivery system, and organ-on-a-chip. In this review, the latest achievements of SFAs applied in biomedical fields are summarized. The authors start by introducing the fabrication techniques of SFAs, then shift to the topology design of SFAs, followed by their material selections and distinct actuating mechanisms. After that, their biomedical applications are categorized in practical aspects. The challenges and prospects of this field are finally discussed. The authors believe that this review can boost the development of soft robotics, biomimetics, and human healthcare.**

## 1. Introduction

Actuators refer to a class of materials and devices with the capability of generating motions or morpho shaping either spontaneously or in response to external stimuli.[1–8] Actuation is an extremely widespread phenomenon in nature organisms and is essential to various life activities. Many plants exhibit actuating behaviors through microscopic stimuli-responsive changes of specialized cells.[9–11] For instance, the leaves of Mimosa droop rapidly when touched;[12] pinecones could switch between opening and closing states, which is caused by the humidity responsive structure of internally oriented cellulose fibrils.[13] In animals and organisms, active motions are more universal and complicated, which typically involve the coordination of nanoscale motor proteins and control systems.[14,15] Taking inspiration from this, artificial actuators that could realize flexible motions have emerged. In contrast to conventional electromechanical actuators, power-free actuators draw significant attention in recent years.[15–17] The actuation mechanism generally includes the accumulation of molecular conformational changes into large shape or volume changes of the actuating material. Besides, these actuators could be endowed with specific structures and respond to various stimuli. Therefore, they are highly promising in miniaturization and controllability, and thus extraordinarily attractive in the field of sensors, robotics, optical systems, and biomedical devices.[14,18–22]

Particularly, the rapid development of the biomedical area puts higher demands on the design of actuators. Specifically, for utilizing in different biomedical scenarios, the actuators are expected to adapt to dynamic environments and interact with the living interfaces.[23–25] Besides, there exhibits a growing trend of miniaturization for systems used in drug delivery, microsurgery, wearable devices, etc.[26–28] These requirements boost the development of novel actuators with rationally designed geometric configurations and superior flexibility in motion and deformation. Prominently, film actuators are excellent candidates, which combine a thin-film substrate with proper actuating principles. Film actuators are typically composed of responsive polymer and gel, carbon material, paper, etc. and could be fabricated by photolithography, electrospinning, 3D printing, and direct casting.[16,29–31] They could convert various forms of energy, including thermal, light, electric, chemical, and magnetic inputs into mechanical work. Besides, by tailoring the structure and micro/nanopatterns of the film actuators, they could generate asymmetric/anisotropic responses and perform programmable target motions such as folding, twisting, rolling, grabbing, crawling, etc. Moreover, by optimizing the composition of the film substrate, the film actuators and the derived smart devices could exhibit superb biocompatibility and biodegradability. These features, together with the ease of fabrication and the relatively high power-to-weight ratio, make film actuators highly attractive in biomedical applications including tissue engineering, delivery system, soft robotics, and organ-on-a-chip.[32,33]

In this paper, we summarize the recent progress of smart film actuators (SFAs) for biomedical applications, as shown in **Figure 1**. Despite that many comprehensive reviews about soft actuators and their wide-range applications have been proposed, one that specifically focuses on thin-film-typed actuators from a biomedical point of view is still rare, especially regarding to up-to-date researches. Herein, we first introduce

Z. Zhang, Q. Wang, L. Shang
Shanghai Xuhui Central Hospital
Zhongshan-Xuhui Hospital
and the Shanghai Key Laboratory of Medical Epigenetics
the International Co-laboratory of Medical Epigenetics and Metabolism
(Ministry of Science and Technology)
Institutes of Biomedical Sciences
Fudan University
Shanghai 200032, China
E-mail: luoranshang@fudan.edu.cn
Z. Zhang, Y. Wang
State Key Laboratory of Bioelectronics
School of Biological Science and Medical Engineering
Southeast University
Nanjing 210096, China

The ORCID identification number(s) for the author(s) of this article can be found under https://doi.org/10.1002/smll.202105116.

**DOI: 10.1002/smll.202105116**

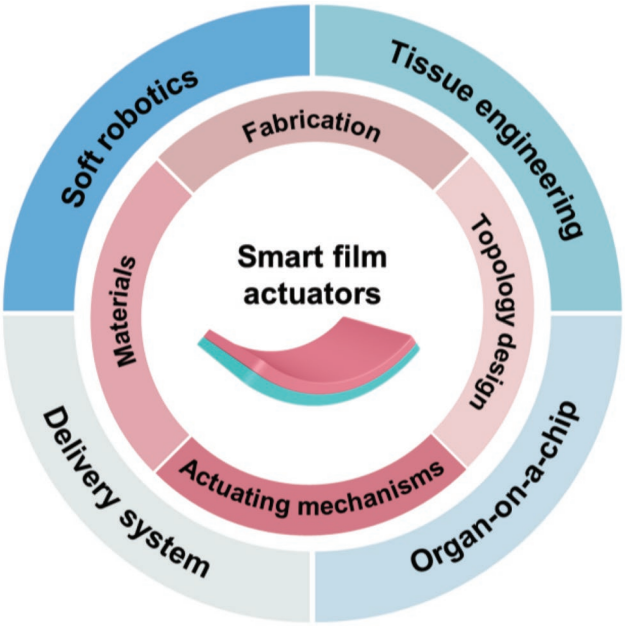


**Figure 1.** Overview of smart film actuators for biomedical applications.

the fabrication of film actuators and discuss how their isotropic/anisotropic and micro/nano topological structures affect their transformation and motion abilities. Next, we categorize the composing materials of the SFAs and the different stimuli-responsive behaviors and various actuating mechanisms of the smart systems triggered physically or chemically. After that, we give an overview of the promising biomedical application of the SFAs in soft robotics, tissue engineering, delivery system, and organ-on-a-chip. Finally, we share our own thinking about existing challenges and future perspectives in this field. We believe this review will help promote the development of advanced SFAs and provide new insight into future biomedical research.

## 2. Fabrication of the SFAs

Various fabrication approaches have been proposed and utilized for the fabrication of SFAs with well-designed structures, functions, as well as application performances. The advances in the field of SFAs indeed benefit from the development of novel manufacturing methodologies. For instance, the advent of photolithography and its ability to tailor polymer materials at the micro-/nano-scale has been transformative for the burst of responsive SFAs, in particular promoting the applications requiring miniaturized soft robotics such as intelligent delivery systems. Additive manufacturing, especially 3D printing, provides another thrust for increasingly complex structural designs. Other commonly-used fabricating approaches, including direct casting, electrospinning, and self-assembly, all contribute to the rapid development of SFAs. Each fabrication approach has its own advantages and limitations, thus it is suitable for specific building blocks and application scenarios, as concluded in **Table 1**. In general, the first step of the fabrication is the tailoring of stimuli-responsive materials by selecting or compositing functional elements, including responsive polymers and gels, carbon materials, magnetic nanoparticles, etc. Then, according to the processibility of different materials, the most appropriate approach is chosen to generate SFAs. Trade-offs exist among various factors, including cost, efficiency, accuracy, optional materials, and structural complexity.

### 2.1. Direct Casting

Direct casting is a popular approach for the fabrication of SFAs due to its low dependency on equipment and perfect technical foundation. It is suitable for easy and rapid prototyping of actuating systems with fixed 3D structures. A large majority of SFAs fabricated by direct casting are generated by catalyst-embedded precursors (mostly silicone). As an example shown in **Figure 2**a, a silicone elastomer pre-mixture is poured over a pre-designed mold, heated, or left for curing, and then peeled off to obtain a film with the shape replicated from the mold.[34] Compared to other fabrication techniques, direct casting generates complex geometrics of SFAs by replicating customized molds, thus saving time and cost. The molds could be fabricated by various methods. For instance, Mosadegh et al. used a fused filament fabrication printer to fast fabricate acrylonitrile butadiene styrene (ABS) molds with a resolution of 300 µm.[35] Since the resolution of SFAs built by direct casting depends on the resolution of the molds, this technique faces the problem of non-evacuated bubbles. These bubbles could be eliminated

**Table 1.** Representative fabrication approaches of SFAs with their advantages and limitations.

| Fabrication technique | Material component | Advantages | Limitations | References |
|---|---|---|---|---|
| Direct casting | Silicon elastomers; thermoplastic polymers | Low equipment dependency; perfect technical foundation; suitable for fast prototyping | Limited by the molds; low resolution | [34–39] |
| Photolithography | Hydrogels | High resolution | Not suitable for fabrication of complex 3D structures | [40–43] |
| 3D printing | Thermoplastic polyurethane-based polymers; silicon-based polymers; hydrogels | Suitable for hierarchical 3D structures; design tailorablity | Low speed | [44–59] |
| Electrospinning | Thermoplastic polymers; hydrogels | High-throughput; suitable for charged and flowable polymers | Restricted by the conductivity of the materials | [60–67] |
| Self-assembly | Cellulose nanocrystal gels; liquid crystal elastomers | Suitable for specific structures | Restricted by the building blocks; Low speed | [31,68,69] |

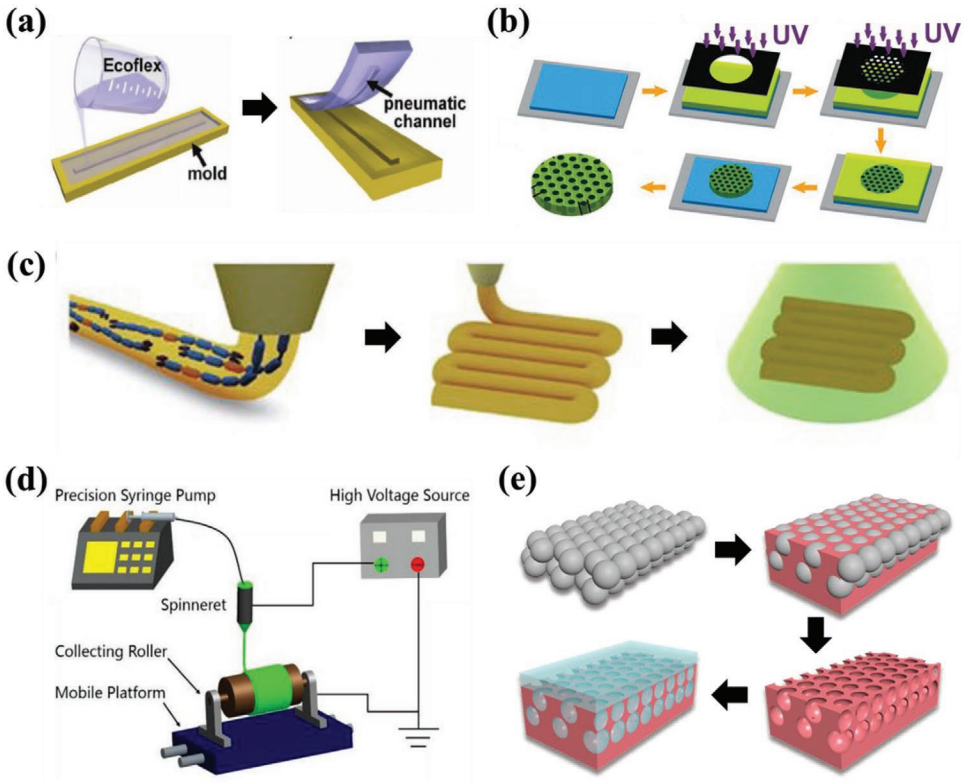


**Figure 2.** Schematic diagrams of various methods for the fabrication of SFAs: a) direct casting; Reproduced with permission.[34] Copyright 2012, Wiley-VCH. b) photolithography; Reproduced with permission.[40] Copyright 2012, American Association for the Advancement of Science. c) 3D printing; Reproduced with permission.[44] Copyright 2020, American Chemical Society. d) electrospinning. Reproduced with permission.[60] Copyright 2018, DMPI. and e) self-assembly replication. Reproduced with permission.[69] Copyright 2019, Wiley-VCH.

by centrifugation[36] and pumping vacuum.[37] Besides, in recent years, to obtain more sophisticated structures, novel casting techniques have been proposed, such as lost wax casting[38] and lamination casting.[39]

### 2.2. Photolithography

Photolithography is a high-resolution manufacturing technique that could transfer predesigned patterns from the photomask to the photoresist on the substrate. The main steps of a typical photolithography process are shown in Figure 2b.[40] First, a photoresist film is deposited on a substrate. Then the sample is illuminated through a patterned mask by light with a certain wavelength, mostly ultraviolet (UV). Photochemical actions occur in the exposed or unexposed area, which depends on the type of photoresists. Thus, the pattern of the mask can be transferred on the resist. Finally, after etching or developing, the photoresist film with predesigned patterns is obtained. This technique can generate complex patterns with high resolution varying from microscales to sub-100 nm scale.[41] Photolithography has been widely used to generate stimuli-responsive hydrogel SFAs with locally interpenetrating networks, allowing elaborate design and construction of asymmetric structures that undergo controlled motions and complicated deformations. A primary pre-gel solution containing monomers and photoinitiators could form hydrogels with interpenetrating networks at the UV light-exposed regions. By further incorporation of functional elements such as liquid metals[42] or 2D materials,[43] the patterned hydrogels can perform various stimuli-responsive shape morphing behaviors predictably and thus serve as SFAs.

### 2.3. 3D Printing

3D printing is a powerful additive manufacturing technology capable of easy fabrication of micro-scaled structures with well-defined distributions in mechanical properties, responsiveness, and functionalities, as shown in Figure 2c.[44,45] It is a promising method to precisely fabricate SFAs with hierarchical 3D deformations and integrate multiple functional materials into single devices. The core feature of 3D printing is the selective layer-by-layer solidification of building blocks (e.g., inks, resins, or powders) to create desired 3D objects. Considering that materials should be both printable and maintain appropriate mechanical features required for actuation, the most commonly adopted materials include thermoplastic polyurethane (PU)-based[46] or silicone-based polymers[47] and hydrogels.[70,71] In recent years, as the technique matures, a growing number of 3D printing approaches have emerged based on inkjet, laser, extrusion, melt electrowriting (MEW), etc., through which a high degree of automation of soft films with actuating capabilities could be fabricated.[48–56] Inkjet printing is a programmed process of depositing ink droplets on the substrate controlled by computers, suitable for the fabrication of responsible hydrogel actuators which are polymerized by UV light.[57] Laser-based

3D printing uses laser powers to discharge and transfer inkjet droplets from the donor layers onto the substrates.[58] The extrusion-based 3D printing squeezes soft polymer filament through a thin nozzle onto the substrates by a pressure source, such as piston, pneumatic pump, or screw.[72] MEW is a high-resolution approach to fabricate complex 3D structures with micro- or nano-scaled fibers. A typical MEW equipment consists of a printing head, a delivery system, and a moving collector. The printing head is equipped with a heater, which could melt the material in the syringe and transfer it to the metal nozzle. The delivery system forces the melted polymers through the nozzle under air pressure and these materials will be driven to the collector under the electrical field.[59,73–75]

### 2.4. Electrospinning

Electrospinning is an efficient technique to fabricate SFAs composed of polymer micro-/nanofibers by using strong electrostatic forces, as shown in Figure 2d.[60] In general, an electrospinning system has three basic components: a high voltage supplier, a spinneret composed of a capillary needle or tube with a small diameter, and a material collecting substrate.[61–64] One electrode is attached to the polymer solution, and the collecting substrate is connected to another electrode or grounded. During the electrospinning process, the polymer solution is charged by high voltage. When the voltage reaches a threshold value, the polymer solution would be ejected from the orifice of the spinneret. The solution jet then undergoes fluid instability and a vigorous whipping process, becoming long and thin. Before reaching the substrate, it evaporates or be polymerized by UV light, transforming into solid fibers and be collected as a membrane scaffold. By now, a variety of SFAs constructed by interconnected micro-/nano-fiber films have been reported.[65,66] It is a versatile method for the mass-production of SFAs from a large number of polymers.[67]

### 2.5. Self-Assembly

Self-assembly is also an effective method for the preparation of SFAs. It could be divided into two types: directly self-assembling into films or replicating self-assembled templates. The former is usually based on the assembly of nanoscale building blocks. For example, cellulose nanocrystals (CNCs) or liquid crystal mesogens could form cellulose nanocrystal gels or liquid crystal elastomers that show responsive behaviors.[31,68] In the latter case, a template film is first prepared by self-assembly of colloidal nanoparticles. Then a pre-polymer solution is poured onto the template and infiltrated the interstices between the colloids. After crosslinking or curing, the template is removed and a flexible film with the negative structure could be obtained. A typical example of the SFA fabricated by replicating self-assembled templates is reported by Zhang et al., as shown in Figure 2e.[69] Silica nanoparticles were assembled into close-packed colloidal crystal nanostructures on a substrate. Then two thermo-responsive polymers were incorporated to replicate the colloidal crystal templates, resulting in a bilayer hydrogel actuator with interconnected interfaces and unique optical properties.

## 3. Topology Design of the SFAs

The driving force of SFAs is the transformation of accumulative dimensional changes of stimuli-responsive building blocks into macroscopic motions. Therefore, the structural design of SFAs is crucial for their actuating performances. For soft materials with isotropic structures, which could contract or expand homogeneously and experience volume change under homogeneous external stimuli, the application fields are relatively restricted. To generate complex deformations or movements, a variety of strategies have been adopted by inducing nonuniform stimuli including localized light irradiation, magnetic field, and electric field to isotropic smart materials.[76–80] Besides, with the development of topological designs, SFAs with anisotropic structures that generate 3D motion and perform complex tasks under both uniform and non-uniform stimuli are becoming increasingly popular. Herein, we introduce the SFAs with anisotropic structures, including bilayer structure, oriented structure, patterned structure, and others.

### 3.1. Bilayer Structure

Bilayer film actuators typically consist of two soft films with different stimuli-responsive construction/expanding rates, as shown in **Figure 3**a.[29] Considering most hydrogels or elastomers have isotropic interconnections, and would expand or contract homogeneously, constructing bilayer film structures is an easy and effective way to generate anisotropic deformations. Due to the difference in the response time or ratio between the two layers, the bilayer material will bend toward the more sensitive layer. The bending degree of the bilayer films could be further adjusted by tuning the thickness ratio of the two layers. Therefore, by designing different patterns, SFAs with bilayer structures could perform complex shape deformations. For instance, Zheng et al. reported a bilayer actuator system composed of two different polymer hydrogels, which have opposite thermo-responsiveness, as shown in Figure 3b-i.[81] When the environmental temperature increased, the bilayer hydrogel strip would bend toward the swelling layer. Then they further fabricated a series of flower-shaped materials, whose petals could close under temperature stimulus, just like a real flower. Thus, these bilayer actuators could serve as grippers and grasp light subjects at a certain temperature. In other cases, bilayer SFAs with designed patterns could perform intriguing deformations such as push-ups, sit-ups, and crawls.[82]

In general, the two layers of bilayer SFAs could be fabricated separately using direct casting or photolithography. During the generation process of the second layer, the pre-polymer solution of hydrogels or elastomers could slightly penetrate the polymer networks of the first layer, resulting in the formation of a thin interpenetrated network at the interface of the two layers, as shown in Figure 3b-ii.[81] Such an interpenetrating interface could enhance the connection of the two layers, making them attached tightly during the reversible bending/unbending process. Besides, chemical bonding is also used to connect the two layers tightly, such as covalently crosslinked interactions.[85]

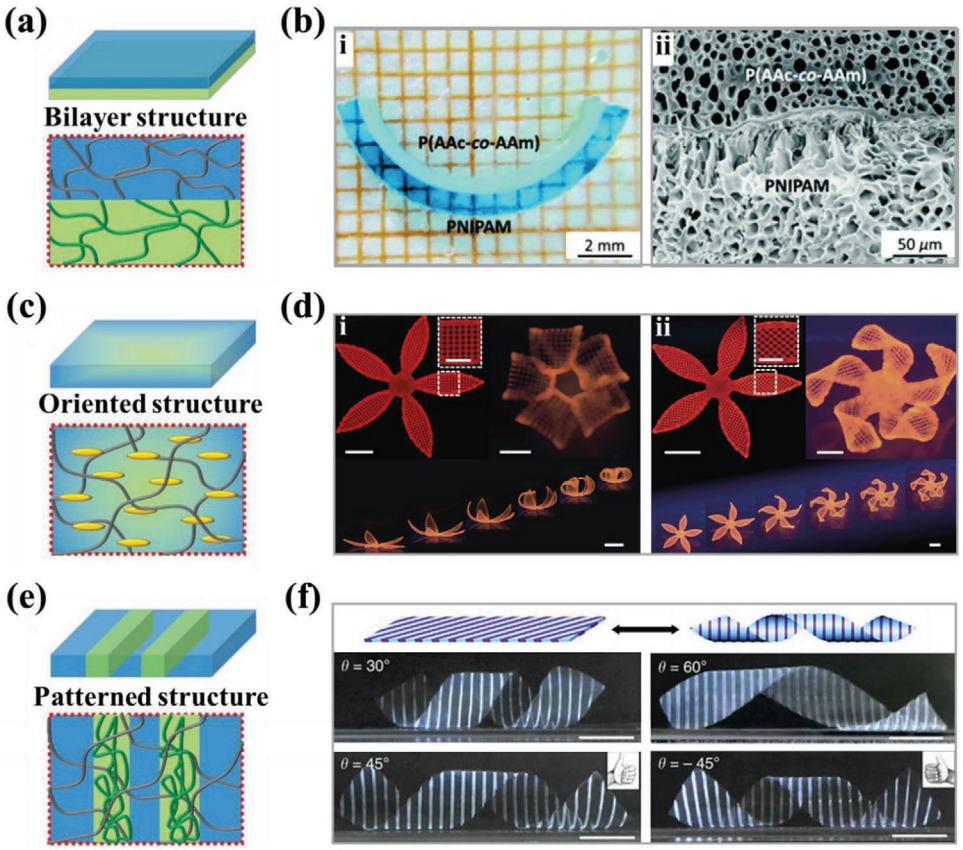


**Figure 3.** a) Schematic diagram of SFAs with bilayer structure. Reproduced with permission.[29] Copyright 2019, Wiley-VCH. b-i) The photograph image and b-ii) the scanning electron microscopy (SEM) image of a bilayer thermo-responsive hydrogel SFA. Reproduced with permission.[81] Copyright 2018, The Royal Society. c) Schematic diagram of SFAs with oriented structure. Reproduced with permission.[29] Copyright 2019, Wiley-VCH. d) 3D printed anisotropic flower-shaped actuators constructed by shear force-induced anisotropic cellulose fibrils with different orientations. Reproduced with permission.[83] Copyright 2016, Springer Nature. Scale bars are 5 mm, inset = 2.5 mm. e) Schematic diagram of SFAs with patterned structure. Reproduced with permission.[29] Copyright 2019, Wiley-VCH. f) Schematic diagram and photograph images of patterned film actuators fabricated by two different polymer composites with helix formed deformation under external stimuli. Reproduced with permission.[84] Copyright 2013, Springer Nature. Scale bars are 1 mm.

### 3.2. Oriented Structure

To impart SFAs with abilities of oriented motion/deformation, it is efficient to construct materials with internal structural orientation. These materials could be constructed by incorporating nanofillers with oriented distributions, such as CNCs or long-chain polymers, as shown in Figure 3c. Shear forces and oriented electric or magnetic fields are often applied to assemble the nanofillers, and then these ordered arrangements could be fixed by solidifying the polymer matrix.[30] Inspired by pinecones in nature, various SFAs with similar structures have been developed. Gladman et al. reported a bioinspired printed hydrogel system by dispersing cellulose nanofibrils (CNFs) into acrylamide (AAm) pre-gel solutions.[83] During the 3D printing process, the CNFs tended to arrange along the direction of the shear force. Compared to the transverse direction, the longitudinal direction showed a different extent of swelling behavior. This property resulted in the anisotropic bending of the printed grid scaffold, as shown in Figure 3d. In another research, Kim et al. presented an SFA with anisotropic electrostatic repulsion due to the presence of internally oriented electrolyte nanosheets. The actuating system was fabricated by the thermo-responsive poly(N-isopropylacrylamide) (PNIPAM) hydrogel doped with unilamellar titanate nanosheets (TiNS). During the polymerization of the PNIPAM hydrogel, an external magnetic field was applied that resulted in a cofacial orientation of the TiNS. When the composite material was triggered by temperature variation, the electrostatic permittivity of the thermo-responsive hydrogel changed, which led to the change of the electrostatic repulsion between the nanosheets and eventually resulted in the variation of the plane-to-plane spacing between the TiNSs. Based on this, an L-shaped actuator was fabricated containing an oblique configuration of the TiNSs. During a cyclic heating-cooling process, the actuator could show unidirectional walking.

### 3.3. Patterned Structure

Patterned SFAs are anisotropic film materials with physically or chemically distinct regions. They could be fabricated by multi-step photolithography with several pre-designed photomasks, and often involve different polymer compositions, as shown in Figure 3e.[29,86,87] Wu et al. designed a monolayer SFA with periodic strips composed of two composite polymer hydrogels, as shown in Figure 3f.[84] These alternant fiber-like regions exhibit different

swelling/shrinking ratios as well as elastic moduli, imparting the material with the ability of anisotropic deformation under external stimuli. To investigate the relation between the internal architecture of the SFAs and their deformations abilities, they designed and fabricated a series of patterned films with different oblique angles of stripes. The resultant actuators could undergo preprogrammed 3D transitions to cylindrical and conical helices.

Apart from introducing multiple polymer composites, patterned SFAs could be constructed just by using a single hydrogel system yet with regional differentiated crosslinking density. Kim et al. proposed a "halftone gel lithography" technique to precisely control the degree of polymerization of polymer composites in different regions.[40] They used two different photomasks and fabricated a patterned hydrogel film with highly crosslinked dots and lightly crosslinked matrixes. The distinct crosslinking density led to a regional swelling discrepancy of the materials, resulting in sophisticated 3D transformations.

### 3.4. Others

Instead of the bilayer, oriented and patterned structures mentioned above, other structures of SFAs have also been constructed to generate 3D deformations/motions. Luo et al. reported a sensitive SFA with a gradient porous structure benefiting from the hydrothermal process of a heterobifunctional crosslinker used.[88] Due to the shape-changing difference of the anisotropic gradient internal structure, the hydrogel film could perform rapid thermo-responsive folding/unfolding deformation. Similarly, Tan et al. developed a thermo-responsive PNIPAM/Laponite gradient SFA using a facile electrophoresis approach.[89] During the polymerization of the PNIPAM hydrogel scaffold, the Laponite migrated toward the anode under an electric field, resulting in the gradient distribution of Laponite in the resultant film. This actuating system exhibited reversible bending/unbending deformation capability, which was attributed to the graded forces generated by the anisotropic swelling/shrinkage of the gradient internal structures.

Alternatively, a novel route to the fabrication of SFAs with complex architectures and ideal transformations has been proposed through modular assembly. Inspired by Lego toys, Ma et al. utilized macroscopic supramolecular recognition to connect hydrogel building blocks as responsive anisotropic actuators.[90] Under pH stimuli, the Lego hydrogels exhibited complex 3D transformation. Besides, the building blocks could disassemble under the change of the oxidation state, and reassemble into completely new composites as required. Yao et al. reported an easy and facile strategy of constructing assembled smart hydrogels by combining diverse hydrogel subunits.[91] These hydrogel subunits with different stimuli-responsive properties were connected by rearranging strong hydrogen bonds between polymer chains and clay nanosheets. Such strategies of assembling responsive blocks according to actual deformation requirements greatly extended the scope of SFAs' structural design.

## 4. Materials of the SFAs

The commonly used building block materials for the construction of SFAs include hydrogels, shape memory polymers (SMPs) and liquid crystal polymer networks (LCNs). Each of the categories exhibits some general properties. Hydrogels are 3D scaffolds formed by hydrophilic polymer chains imbibed with abundant water molecules. Due to their high content of water, they are particularly appealing to biomedical applications.[92–96] SMPs are a type of polymers that can transform into temporary shapes and restore their permanent shapes by external stimuli.[97] They are not limited to pure polymeric systems but also include polymer blends and composites, with superb mechanical and physical properties such as stiffness, rigidity, and flexibility.[98] Owing to the reduction or activation of internal molecular chain mobility, SMPs could be actuated under a solvent-free environment. LCNs are polymer networks consisting of mesogens self-assembled into liquid crystalline phases. LCNs could also work under solvent-free conditions.[99,100] Due to their internal local order, liquid crystal polymers are imparted with low coefficients of expansion and high modulus.[101] Crosslinked liquid crystal polymers, or LCNs, could exhibit anisotropic extraction/contraction along the alignment direction of the mesogens.[102]

Besides, in order to expand the functionality of the building blocks mentioned above, functional elements are chosen and incorporated into the material systems. These elements can be categorized into polymers and nanomaterials. Some polymers could co-crosslink with the building blocks to impart the system with the capability of stimuli-responsive volume change.[103–106] This is commonly achieved through chemical reactions between functional polymers and environmental chemicals or based on intermolecular reactions under stimulation of physical parameters such as temperature variation. On the other hand, some nanomaterials have unique photothermal or electrothermal properties and could convert light or electrical energy into internal energy, thus triggering anisotropic deformation.[107–114] Some magnetic nanomaterials can drive the SFAs under the force of the magnetic field.[115–121] The mechanism of these responsible actuations are discussed in detail in the next section.

## 5. Actuating Mechanisms of the SFAs

In recent years, SFAs have been widely studied due to their merits of flexibility and adaptability compared to traditional rigid robots.[122] Some of the design principles originate from the abundant examples of living actuating systems in mother nature, including animals, plants, and microorganisms.[123–125] Their soft features impart them with great potential to perform complicated forms of movement and deformation. Particularly, a variety of "smart" responsive materials have been exploited; they could undergo changes in volume, hydrophilicity/hydrophobicity, conformation, or solubility in response to external stimuli such as temperature, humidity, light, chemicals, and electricity or magnetic field. Recent years have witnessed significant progress in the development of stimuli-responsive SFAs by combining these smart materials with facile structural design through advanced fabrication techniques. In this section, we categorize the stimuli mechanisms of SFAs based on different external stimuli.

### 5.1. Thermo-Actuation

Among the smart actuating systems, thermo-responsive polymers are by far the most widely studied. These materials have the capability to undergo volume/solubility transitions reversibly in response to temperature changes in their surrounding environments. Typically, thermal-responsive materials are networks combined by hydrophobic groups (e.g., methyl, ethyl, and propyl) and hydrophilic groups (e.g., amide or carboxyl).[103] These polymer networks exhibit a transition point, namely the lower critical solution temperature (LCST) or upper critical solution temperature (UCST).[104–106] In the aqueous solution with a lower temperature than LCST, the LCST-type polymers have a swelling state and an extended state due to the extensive hydrogen bonds formed between the polymer networks and water molecules. When the solvent temperature is higher than LCST, the polymer networks would release water molecules due to the increase of system entropy and the break of hydrogen bonds, thus leading to a shrinking and collapsed state. In contrast to the LCST-type polymers, the UCST-type polymers expand when the solvent temperature is higher than UCST and shrink when the temperature is lower than UCST.

PNIPAM, first reported in 1967 by Scarpa et al.,[126] is the most extensively used thermo-responsive polymer (**Figure 4**a). When heated to its LCST (≈32 °C) in an aqueous solution, which is close to the physiologically relevant temperature, it undergoes a transformation from coil state to globule state. A great number of works have been reported for the adjustment of the phase transition temperature of PNIPAM to meet the needs of practical applications. To this end, other hydrophobic or hydrophilic monomers, such as AAm and acrylic acid (AAc) could be introduced to form copolymer networks.[127,128] Generally, PNIPAM-based SFAs are designed with a bilayer or gradient structure.[129] Hu et al. reported the bilayer-structured PNIPAM hydrogel actuator by incorporating a temperature inert polyacrylamide (PAAm) layer. When the temperature exceeded 38 °C, the PNIPAM layer shrunk and caused the PAAm layer to bend into a circle. Inspired by this work, a lot of PNIPAM-based actuators emerged to yield fast, reversible and complex actuations. For instance, Xiao et al. reported a bilayer thermo-responsive hydrogel composed of a PNIPAM layer and a poly(3-(1-(4-vinylbenzyl)-1H-imidazol-3-ium-3-yl)propane-1-sulfonate) (PVBIPS) layer.[130] They fabricated the bilayer actuator by a facial one-pot method to copolymerize the incompatible NIPAM and VBIPS, which is a UCST monomer (Figure 4b). The resultant two layers had opposite thermo-responsiveness and experienced different swelling/shrinking behavior under heating or cooling. A gripper designed based on such PNIPAM-PVBIPS bilayer film showed a fast and reversible bidirectional bending behavior, and could capture, transport, and release cargos under the control of temperature variation. In another intriguing example, Liu et al. reported a thermo-responsive hydrogel fabricated just by PNIPAM itself.[131] The actuator was composed of an orderly arranged PNIPAM fiber composite layer and a randomly arranged PNIPAM fiber composite layer, as shown in Figure 4c. When the solvent temperature varied, the material could change its 3D conformation along with the orientation of the ordered PNIPAM fibers attributing to the asymmetric swelling of fibers in both layers.

Apart from thermal-responsive hydrogels, thermally activated SMPs are another type of material feasible for the construction of SFAs. Thermally activated SMPs change their shapes according to reversible variations in polymer chain mobility with ambient temperature. The most commonly used switching temperature ($T_{trans}$) of SMPs are glass transition temperature ($T_g$) and melting temperature ($T_m$).[133] For example, Jin et al. designed an SMP-based SFA using crystalline PU networks ($T_m$ = 50 °C) with thermo-reversible bonds. With the aid of the origami method, the resultant material could be formed into various 3D patterns with reversible shape memory capabilities.[132] A 3D crane was further fabricated and showed reversible wing flapping motions triggered by environmental temperature variation, as shown in Figure 4d.

### 5.2. Light Actuation

Light-responsive actuators have attracted much attention mainly because they could be remotely triggered and controlled by tuning the location and/or intensity of the radiation. This feature is desirable for some special application scenarios, such as remote surgery and soft robotics. Traditional light-responsive polymers incorporating chromophores (e.g., azobenzene, dithienylethene, and pyrenylmethyl ester) that can absorb light at specific wavelengths and undergo chemical reactions or conformational changes.[134,135] Although widely reported, the inferior biocompatibility and biodegradability of these materials greatly limit their applications in the biomedical field.[135–137] In view of this, SFAs driven by photo-thermal agents have been attracting tremendous attention due to their superior material selectivity, machinability, and manipulability. These actuating systems are typically constructed by compositing thermo-sensitive scaffolds and light-absorbing elements. With the incorporation of photothermal agents, including inorganic and organic ingredients, the composite system could absorb light and convert it into heat and eventually undergo responsive deformation.[107–113] SFAs prepared based on different classes of photothermal agents have their own advantages, disadvantages, and application scenarios. Among them, near-infrared (NIR)-absorbing photothermal agents have gained a unique position in biomedical applications, because NIR could penetrate tissue deeply.[138] The commonly used NIR absorbing photothermal agents include carbon nanotubes (CNTs), graphene oxide (GO), and MXenes. Herein, we discuss some typical works of SFAs based on these nanomaterials.

CNTs are widely used in preparing responsive SFAs due to their outstanding photothermal conversion performance in the visible and NIR range, strong mechanical strength, and brilliant thermal conductivity (**Figure 5**a).[139,140] There is evidence that polymers doped with CNTs could gain better mechanical strength, tensile property, and stability.[141] Accordingly, CNT-based SFAs have demonstrated deformation ability, robustness, and a long lifetime. Recently, Hua et al. fabricated a paper-based bilayer actuator composed of multi-walled CNTs (MWCNTs) and polylactic acid (PLA) using the 3D printing technique.[142] This actuator showed fast, remarkable, and reversible deformation mainly due to the good NIR absorption of MWCNTs and the fast thermo-responsiveness of PLA when heated to the

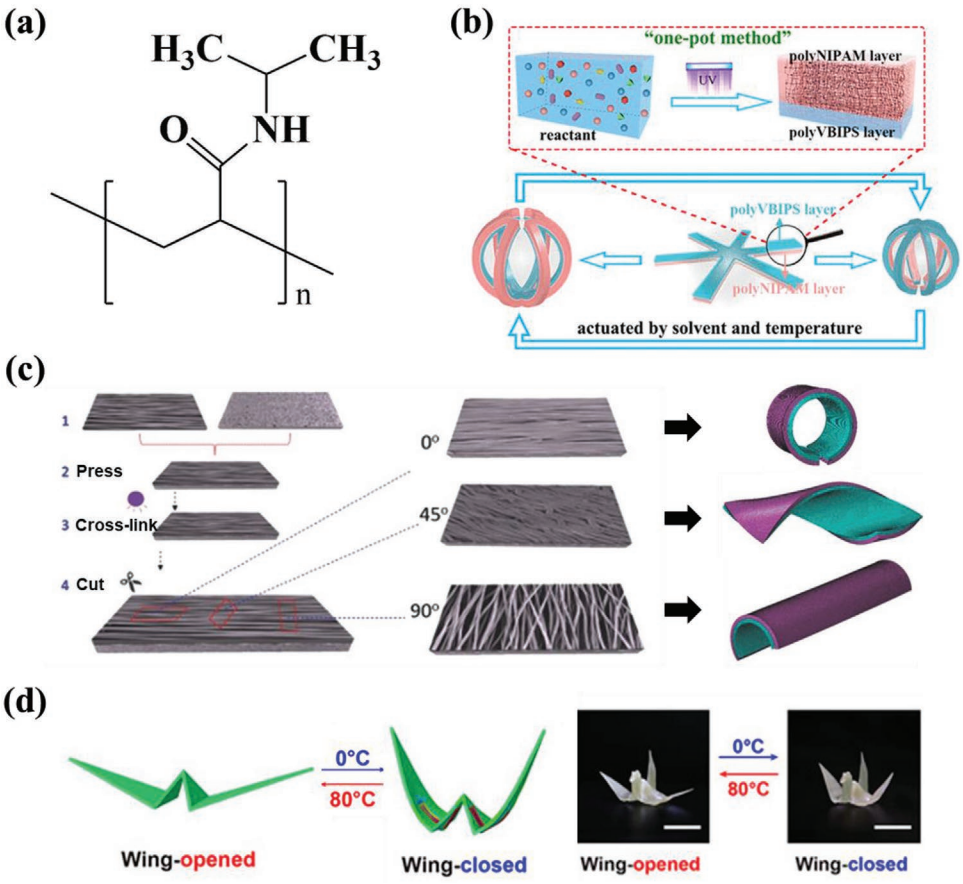


**Figure 4.** a) Chemical structure of the PNIPAM monomer. b) Schematic diagram of the preparation and working mechanism of the PNIPAM-PVBIPS bilayer hydrogel. Reproduced with permission.[130] Copyright 2018, American Chemical Society. c) Schematic diagram of the preparation and working mechanism of the anisotropic PNIPAM bilayer hydrogel with different internal PNIPAM fiber orientations. Reproduced with permission.[131] Copyright 2016, Wiley-VCH. d) Schematic and images of the reversible wing-flapping of a crane-shaped 3D SMPs actuator triggered by temperature variation. Reproduced with permission.[131] Copyright 2018, American Association for the Advancement of Science. Scale bars are 1 cm in (d).

$T_g$ (Figure 5b). In another study, Peng et al. embedded aligned CNTs (ACNTs), which were assembled under van der Waals forces, in paraffin wax (PW) to construct a bilayer photothermal actuator with polyimides.[143] Since the transverse modulus of ACNTs was lower than their longitudinal modulus, when exposed to NIR light, the PW tended to bend perpendicularly to the alignment orientation of the ACNTs, causing the polyimide layer to bend synchronously. Therefore, by adjusting the alignment orientation of the ACNTs, the paraffin/ACNTs-polyimides bilayer actuator showed phototropic, apheliotropic, and even helical bending behaviors under NIR irradiation.

Graphene is a typical 2D carbon material with entire $sp^2$ hybrid bonds, and exhibits brilliant photothermal conversion performance and ultralight weight. Graphene has been widely used in the development of SFAs (Figure 5c).[146,147] Taking advantage of this property, Niu et al. reported a sensitive light-driven bilayer SFA by coupling pristine polydimethylsiloxane (PDMS) layer and a composite PDMS layer doped with graphene nanosheets.[148] Under NIR irradiation, the temperature of the bilayer film could rise to 60 °C within 5 min, which resulted in the bending of the film toward the composite layer. However, the hydrophobicity of graphene greatly limited its further application.[149] Consequently, many graphene derivatives, such as modified sulfonated graphene, GO, and reduced GO (rGO) have been explored in preparing SFAs.[150,151] In a recent research, a PNIPAM/GO-P(AAm-*co*-AAc) bilayer actuator was constructed with a flower-like shape, as shown in Figure 5d.[69] The two hydrogel layers showed opposite thermo-responsiveness; as a result, the bilayer actuator would bend toward the PNIPAM/GO layer when heated. Under the remote control of NIR light, the flower-shaped actuator could perform closing/capturing and opening/releasing deformations.

MXenes are a class of 2D nanocrystals first reported in 2011, and it opens a door to a large number of 2D functional nanomaterials (Figure 5e).[145,152] The general formula of MXenes is $M_{n+1}AX_n$, where M is an early transition metal, A is the surface termination group, and X is carbon and/or -nitrogen. Among many features of MXenes, such as high electrical conductivity, moderate Young's modulus and brilliant thermal conductivity, the most attractive one is their ultrahigh photo-thermal conversion efficiency (about 100%).[153–155] This excellent property makes MXenes highly applicable to preparing light-driven SFAs. For example, Cai et al. fabricated a bilayer film actuator based on the combination of $Ti_3C_2T_x$ MXene-cellulose composites (MXCC) and polycarbonate (PC) films.[156] Under NIR irradiation with an illumination intensity of 80 mW $cm^{-2}$, the

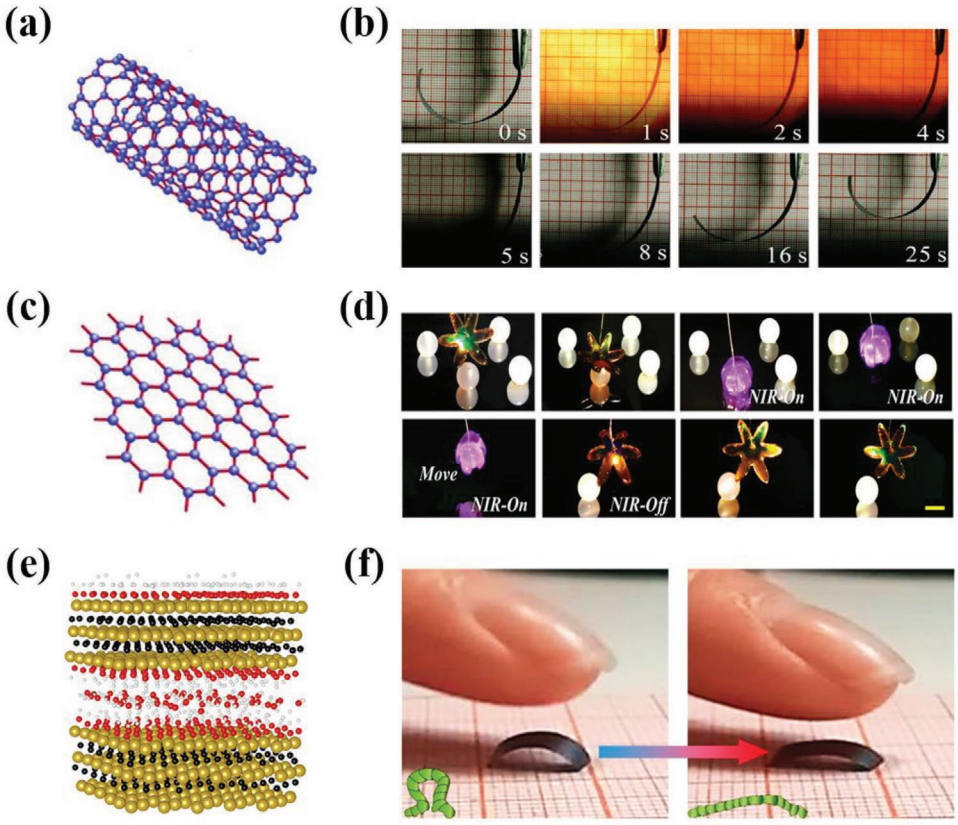


**Figure 5.** a) Lattice structure of CNT. Reproduced with permission.[144] Copyright 2018, Wiley-VCH. b) The bending and recovering of the MWCNTs-PLA bilayer actuator triggered by NIR irradiation. Reproduced with permission.[142] Copyright 2018, The Royal Society. c) Lattice structure of graphene. Reproduced with permission.[144] Copyright 2018, Wiley-VCH. d) The closing/ capturing and opening/releasing deformations of the flower-shaped PNIPAM/GO-P(AAm-*co*-AAc) bilayer actuator remotely triggered by NIR light. Reproduced with permission.[69] Copyright 2019, Wiley-VCH. e) Atomistic model of the structure of $Ti_3C_2T_x$ MXene. Reproduced with permission.[145] Copyright 2011, Wiley-VCH. f) Optical images of the crawling of the inchworm-shaped PW-MXene actuator triggered by infrared irradiation of a human finger. Reproduced with permission.[110] Copyright 2021, American Chemical Society.

MXCC/PC bilayer actuator could be locally heated and exhibit a large-angle bending (169°) within 6.5 s. Alternatively, Xiao et al. reported a composite film actuator based on PW and $Ti_3C_2T_x$ MXene with a gradient structure. This structure was generated by penetrating an MXene membrane using melted PW. The as-prepared film actuator showed sensitive photo-thermal transition properties and could crawl like an inchworm under the trigger of infrared irradiation of human bodies, as shown in Figure 5f.[110]

### 5.3. Electro-Actuation

Electro-responsive SFAs use electro-responsive polymers or electrothermal conversion agents to realize deformations/motions under electrical stimulation. By doping electrothermal conversion agents (e.g., CNTs and GO) in thermo-responsive polymer networks, the composite material could be heated under electric fields and show anisotropic morpho shapes.[114] Besides, electro-responsive polymers, including ionic types and electronic types, account for a large portion of electro-responsive SFAs. Ionic type polymers, including conducting polymers (CP), ionic polymers (IP), and IP metal composites (IPMCs), are generally used in wet conditions with low triggering voltages, and exhibit small deformation and slow response. Among them, IPMCs generally show a larger range of deformation and better physical/chemical stabilities, and thus are widely used.[60] When applying an external electric field, the electrostatic force would drive the directional movement of hydrated mobile ions, and this is usually accompanied by solvent entrainment and network expansion/collapse, thus realizing anisotropic actuating.[104] Wang et al. constructed an ultrathick IPMC actuator with nanodispersed metal electrodes. Briefly, ultrathick ion-exchange membranes were generated by stacking multi-layer Nafion films with the metal electrodes constructed on the membranes through alcohol-assisted electroless plating (**Figure 6**a).[157] The as-prepared film actuator could lift a 124 g cargo for 90 s under stimulation of 4 V DC, with a height of 25 mm (Figure 6b).

Electric-type electro-responsive SFAs, which have the characteristics of large deformation and fast response under high voltage and dry working environments, are commonly fabricated by sandwiching dielectric elastomer (DE) films with compliant electrodes.[104] Under voltage stimulation, reversible compression in thickness and lateral expansion of the DE films between electrodes could be performed under the action of Maxwell stress.[158] Shian et al. reported a typical DE bending SFA fabricated by sandwiching an acrylic elastomer film between two single-walled CNT electrode layers.[159] They imparted the DE-based SFA with local stiffness by incorporating oriented fibers into the elastomer film,

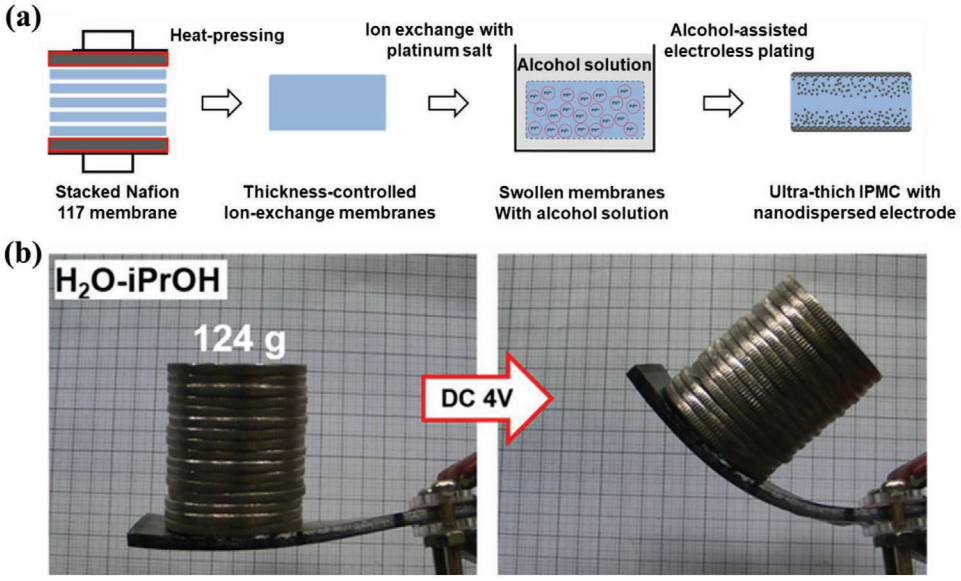


**Figure 6.** a) Schematic diagram of the fabrication of the ultrathick IPMC actuator based on thickness-controlled ion-exchange membranes with nanodispersed metal electrodes. Reproduced with permission.[157] Copyright 2017, American Chemical Society. b) Actuation of the IPMC film under 4 V DC. Reproduced with permission.[157] Copyright 2017, American Chemical Society.

affecting its strain capacity in different directions. The resultant material can therefore bend in a directional way under electric stimulation, serving as a gripper and capturing cargos.

### 5.4. pH-Responsiveness

pH-responsive SFAs are generally fabricated by incorporating pH-responsive monomers into polymer networks, and could be divided into two categories: ionizable-types or acid-cleavable-type. Ionizable polymers usually consist of weak acids and/or bases that can be ionized by controlling the pH of the solution to produce polyanions, polycations, and polyzwitterions. The most widely used pH ionizable SFAs are composed of AAc, methacrylic acid, boronic acid (BA), amine-containing functional groups, and their derivatives.[160–164] For the anionic monomers, when the pH exceeds their unique dissociation constant (p*K*a), the polymer networks would undergo a transition of solvation state and conformation, resulting in the variation of volume.[104] By contrast, for the cationic monomers, once the amine groups are protonated, they would be positively charged. The polymers consisting of acid-cleavable groups can undergo acid and/or base induced cleavage to produce a charged state.[104] When the external pH value changes, the degree of dissociation of these groups changes accordingly, resulting in the variation of ion concentration inside and outside the material, as well as the ion interaction force. On the other hand, the dissociation of these groups will also destroy the relevant hydrogen bonds in the polymers, resulting in changes in the number of cross-linking points in the polymer network and the structure of the materials. Based on this principle, many SFAs can be designed to be deformed under pH stimulation, and work in senarios that pH need to be measured in small volumes, either in vitro or in vivo.

In a typical work reported by Han et al., a bilayer hydrogel was constructed by coupling a PAAm layer and a PAAc layer.[165] **Figure 7**a-i shows the swelling behavior of the two pH-responsive polymer hydrogels in a series of aqueous solutions with different pH values. Due to the difference in swelling ratio, the resultant PAAc-PAAm bilayer hydrogel was endowed with a bidirectional bending ability in both acidic and alkaline solutions. The bending direction of the actuator could be simply regulated by pH value, as shown in Figure 7b-ii,b-iii. In another intriguing work, Li et al. reported a bilayer SFA constructed by coupling a 2-hydroxyethyl methacrylate (PHEMA) layer with a poly(ethylene glycol)diacrylate (PEGDA) layer doped with iron oxide particles ($Fe_3O_4$), as shown in Figure 7b-i.[166] The PHEMA layer was employed for pH-triggered folding and unfolding motion and the PEGDA/$Fe_3O_4$ layer was used for the magnetic-controlled locomotion. Under different pH values, the PHEMA layer and the PEGDA layer showed different swelling ratios (Figure 7b-ii). Thus, the flower-shaped soft microrobot could close at a high pH value and open with the decrease of pH (Figure 7b-iii).

### 5.5. Others

In addition to the types of stimuli mentioned above, there are many other actuating triggers for SFAs, such as humidity, magnetic field, and biochemicals. Humidity-responsive SFAs perform swelling-driven 3D deformations depending on the ambient humidity.[167,168] Magnetic-responsive SFAs enforce motions in response to external magnetic fields by embedding magnetic nanoparticles (e.g., $\gamma$-$Fe_2O_3$, $Fe_3O_4$, and $CoFe_2O_4$ nanoparticles) into soft materials.[115–121] The properties of magnetic SFAs rely on several factors, such as the type of the soft polymers and magnetic nanoparticles used, the size and distributions of magnetic nanoparticles as well as their concentrations.[169] The magnetic force exerting on the magnetic nanoparticles drives SFAs in a directional manner. Such remote manipulation capability imparts these materials with

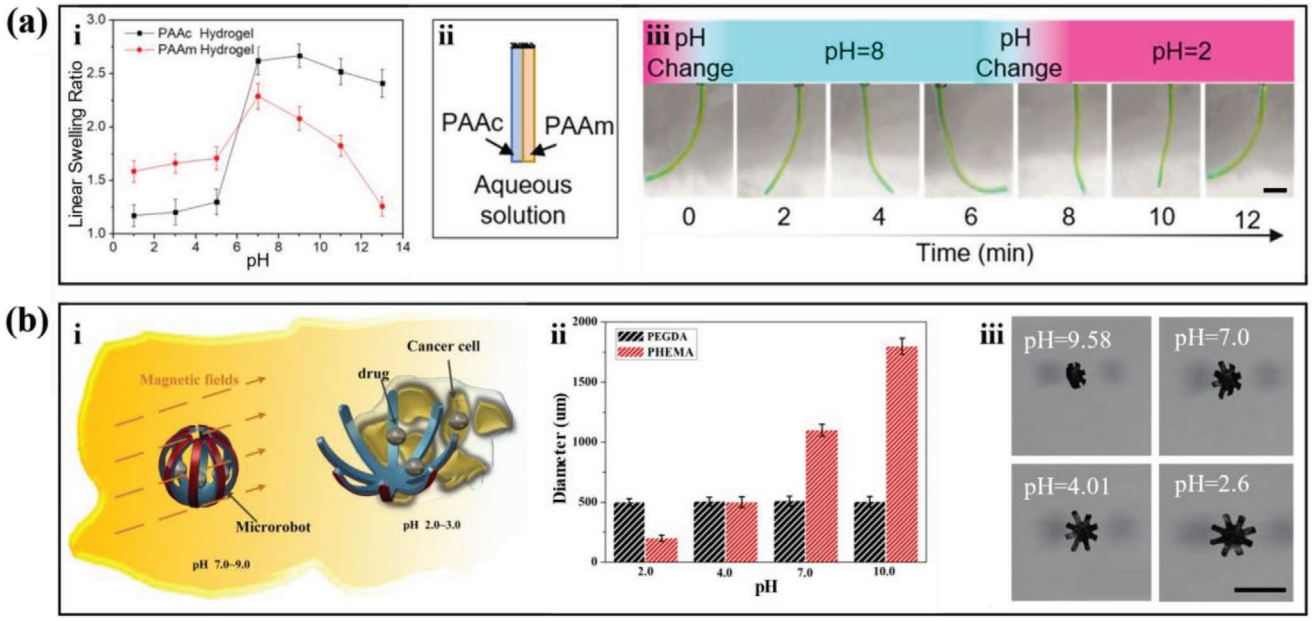


**Figure 7.** a-i) The swelling ratio of the PAAc hydrogel and the PAAm hydrogel as a function of pH value; a-ii) schematic diagram of the PAAc-PAAm bilayer hydrogel; a-iii) a series of images of the bilayer actuator under different pH value conditions. Reproduced with permission.[165] Copyright 2020, American Chemical Society. Scale bar is 2 cm. b-i)Schematic diagram of the working mechanism of the soft actuator, which could move by the magnetic field and perform drug carrying and release by folding/unfolding motions triggered by different pH values; b-ii) a histogram of the expansion ratio of circular PEGDA and PHEMA hydrogels; b-iii) the folding/unfolding motions of the SFA under different pH values. Reproduced with permission.[166] Copyright 2016, IOP Publishing. Scale bar is 3 mm.

great potential for biomedical applications, such as remote surgery and controlled delivery systems. Biochemical-responsive SFAs use specific recognition interactions between functional materials and target biomolecules, such as enzymes or ions, as the actuating trigger to complete complex tasks.[170,171]

## 6. Cutting-Edge Biomedical Applications

The emergence of SFAs brings opportunities to many biomedical areas, and the progress of modern medicine has put forward higher requirements for medical devices, which in turn has promoted the rapid development of SFAs. Since SFAs directly contact with living cells or tissues in biomedical application scenarios, the biocompatibility of the materials is an essential requirement. Not only the responsive polymer framework but also the functional doping nanomaterials are expected to have no cytotoxicity or immunogenicity.[172–174] Besides, flexibilities, tunable microstructures, and sustainability are also important requirements. The most commonly used building block are hydrogels, such as modified PEGDA, gelatin methacrylolyl, and alginate hydrogels. They are attractive in their high water content and 3D scaffold structures, which provide sufficient nutrients and gas supply for cells and tissues.[175] Besides, other functional materials with brilliant biocompatibility are also promising candidates for the construction of SFAs, such as silicon-based polymers and cellulose-based liquid crystals.[176,177] In the premise of good biosafety and biocompatibility, SFAs could be applied to the biomedical field. For example, to meet the demands of minimally invasive surgery, lightweight SFAs yet capable of generating large forces in limited volumes are anticipated.[178] Some medical actuators can reach remote and hard-to-reach tissues of the body, performing diverse medical procedures like robots. SFAs can also be used as a microcarrier for the targeted delivery of drugs or cells in vivo. In addition, actuators based on flexible films have been used for in vitro tissue engineering. When combined with specific sensing units, SFAs can be used for medical applications such as drug screening and single-cell detection. Herein, we introduce the main applications of biomedical SFAs, including soft robotics, tissue engineering, delivery system, and organ-on-a-chip.

### 6.1. Soft Robotics

Soft medical robotics interacts directly with humans at different scales. For example, some of the devices collect tissue samples and/or reduce tissue damage during surgery or endoscopy.[23,179] In particular, the combination of SFAs allows for further miniaturization and more flexible performances of the biomedical soft robotics, thus paving the way for collecting tissue samples in hard-to-reach areas.[180,181] For example, star-shaped soft robotics have been reported that could close down and grasp tissues under the trigger of diverse external stimuli.[182–188] These devices have shown their capability of capturing red blood cells and fibroblasts for single-cell screening (**Figure 8**a).[182,188] Biocompatible designs constructed by responsive hydrogels embedded with alginate magnetic microbeads could be remotely guided by magnetic fields and exhibit NIR-induced single-cell capturing behaviors.[187] Besides, star-shaped microgrippers have been tested in animal models and demonstrated their functionality in retrieving tissues from a porcine bile duct[185] (Figure 8b). The retrieved tissues could be used for the extraction of intact cells as well as quality RNA or DNA, which

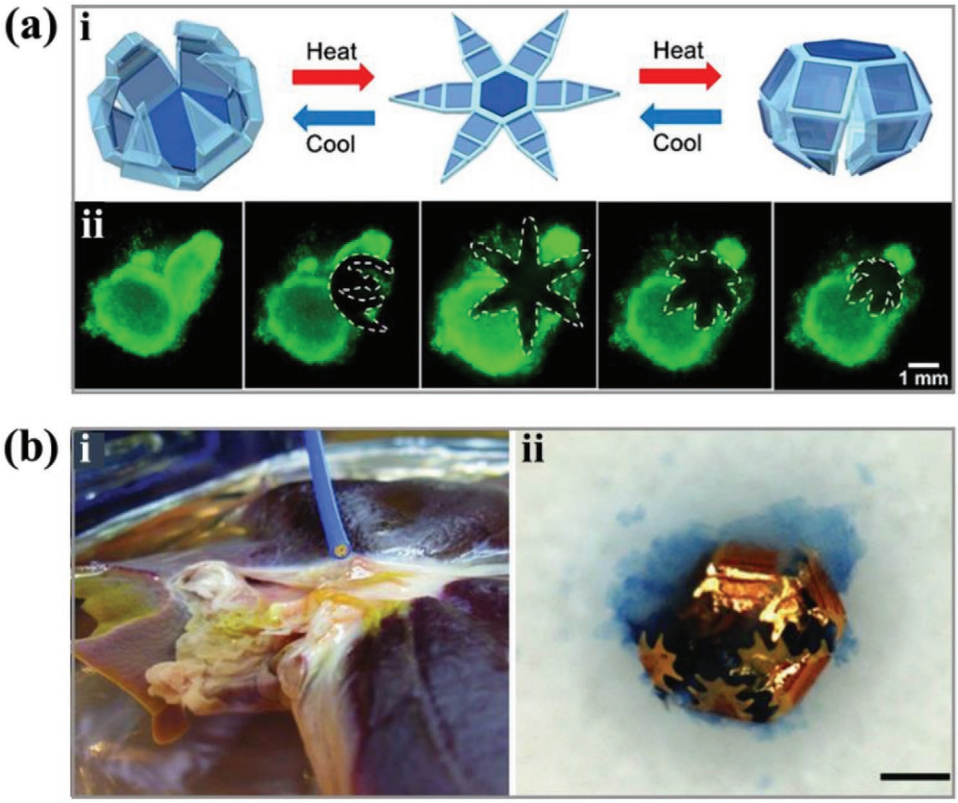


**Figure 8.** SFA-based soft medical robotics. a-i) Schematic diagram of the thermal-actuated soft robotics; a-ii) fluorescent images of the star-shaped microgripper capturing and excising cells from a living fibroblast clump. Reproduced with permission.[182] Copyright 2015, American Chemical Society. b-i) Photograph image of the control of the soft biopsy robotic using a magnetic catheter; b-ii) photograph image of the retrieved robotic with a piece of excised tissue, which was stained in blue. Reproduced with permission.[185] Copyright 2013, Wiley-VCH. Scale bar in (b-ii) is 100 µm.

established a platform for the diagnosis of cancer, inflammatory, or other diseases.

### 6.2. Tissue Engineering

Tissue engineering is a promising technique aimed at repairing diseased or damaged tissues by culturing artificial tissues that mimic natural tissues or organs in structure and function. SFAs, which can undergo 3D deformation under external stimuli, can address the needs of tissue engineering from two aspects: engineering living cells into organized tissue-like patterns through surface topological design; precisely forming artificial tissues with complex 3D configurations. Zhao et al. developed an artificial vascular graft based on poly (lactide-co-trimethylene carbonate) (PLATMC), a degradable SMP, to solve the problems of symbiosis tissue shortage and immune rejection in the treatment of vascular diseases (**Figure 9**a).[189] Human umbilical vein endothelial cells were first randomly seeded on the functionalized nanofiber layer of a 2D scaffold and attached to the scaffold at room temperature. The scaffold was then placed into a 37 °C incubator, allowing the cells to prolificate and differentiate as the film curled. Finally, the endothelial cells were homogeneously distributed on the lumen of the 3D scaffold since the film substrate deformed to its original tubular shape under $T_g$. This study provided a new idea for the construction of advanced vascular grafts. In another example, PLATMC was utilized to construct temperature-triggered multichannel scaffolds (Figure 9b).[190] The flat temporary films cultured with Schwann cells could self-fold into tubular shapes under 37 °C, and exhibit brilliant performance in cell growth and the repairing of rat sciatic nerve defects.

### 6.3. Delivery System

SFAs could undergo shape deformations under external stimuli, thus they can be used as delivery carriers for in vivo therapies. Targeted therapy based on precise delivery of drugs and therapeutic cells is a cutting-edge strategy for autoimmune and degenerative diseases, genetic disorders, and cancer. Given the risk of structural and functional damage to cells and drug agents during the delivery process, it is important to develop effective carriers. SFAs, which can wrap and deliver cargos to target sites and then release them under specific stimuli, have become a research hotspot. For example, star-shaped bilayer SFAs constructed by biodegradable PCL and thermal-responsive PNIPAM-(4-acryloylbenzophenone) hydrogels have been tested promising as delivery carriers (**Figure 10**a).[191] Under the temperature stimuli, they exhibited reversible encapsulation and release of yeast cells. The 4 µm-thick polymer bilayer could complete bending/unbending deformation in 5–10 s. Similarly, based on the unique range of pH and temperature within the gastrointestinal tracts, stimuli-responsive SFAs that could seize the tissue upon deformation and released

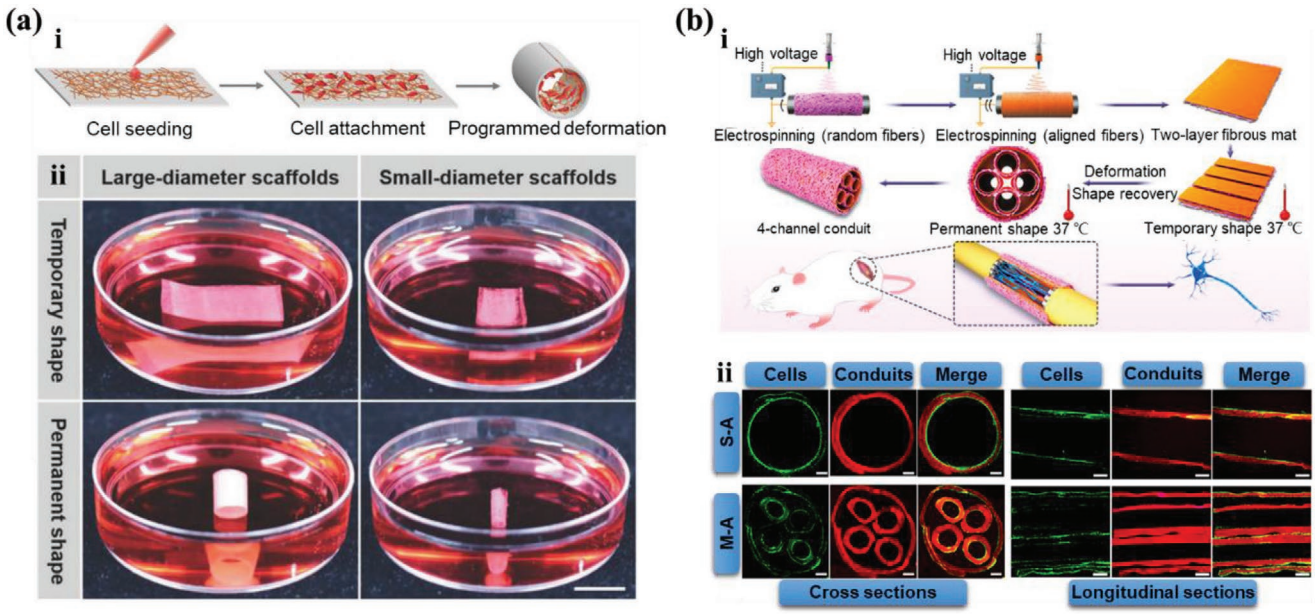


**Figure 9.** SFA-based shape-morphing scaffolds for tissue engineering. a-i) Schematic diagram and a-ii) photograph images of the preparation and deformation of the tissue engineering scaffolds seeded with HUEVCs. Reproduced with permission.[189] Copyright 2018, Wiley-VCH. Scale bar in (a-ii) is 1 cm. b-i) Schematic diagram of the preparation and application of the SFAs-based tissue engineering conduit for nerve repairing; b-ii) fluorescent staining images of the distribution of nerve cells in conduits after culturing for 7 days. Reproduced with permission.[190] Copyright 2020, American Chemical Society. Scale bars in (b-ii) are 400 µm.

drugs from their porous scaffolds have been developed.[192,193] Besides, endoscopic in vivo experiment demonstrated the precise drug release of the food dye in the porcine stomach, proving that these SFAs-based delivery system is promising for clinical conditions (Figure 10b).[193] In addition to achieving precise release in the target area, self-degradation without retrieving is also an important research direction of SFAs-based delivery systems. In a recent work, a thermal-responsive SFA gripper doped with magnetic nanoparticles was demonstrated. It could move to the target place under external magnetic control and release the loaded drugs under body temperature (≈37 °C). More importantly, it could degrade at this temperature due to cleavage of the disulfide bonds by reduction and disappear in 20 days.[194]

### 6.4. Organ-on-a-Chip

Organ-on-a-chip is a technique to construct an organ-like physiological microsystem in vitro, which has been validated as an efficient alternative to traditional animal models in terms of disease modeling, drug screening, personalized medicine, toxicity prediction, etc.[195,196] The key elements of organ-on-a-chip platforms include living cells, tissue interfaces, biological fluids, and mechanical forces. In recent years, SFAs actuated by living cells have been proposed for the study of organ-on-a-chip. As an example, cardiomyocytes cultured on flexible materials could exert forces to deform the material through beating.[175,197,198] Thus, the deformation degree of the material can provide feedback on the physiological conditions of

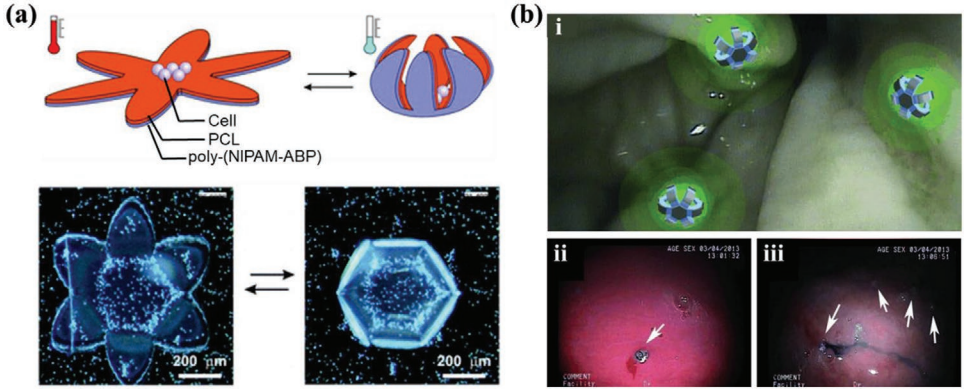


**Figure 10.** Controlled-delivery vehicles based on SFAs. a) Schematic diagram (upper) and photograph images (lower) of a star-shaped thermal-responsive cell delivery SFA. Reproduced with permission.[191] Copyright 2011, Informa UK Limited. b-i) Schematic diagram of the SFAs-based microcarriers attached to a colon wall and the release of green fluorescent drug to the target areas; (b-ii–iii) endoscopic in vivo images of drug-releasing SFAs eluting blue food dye in the porcine stomach. Reproduced with permission.[193] Copyright 2014, Wiley-VCH. Arrows point to the SFAs.

the cells under external stimuli. As a proof-of-concept study, Parker et al. seeded cardiomyocytes onto a PDMS film with surface microgrooves and guided the cells to self-assemble into anisotropic lamellar cardiac tissues along with the 3D structures, mimicking the structure of a natural heart.[199] The stress produced by cardiac lamellar tissues was within the range of 1–15 kPa.[200] Thus, they optimized the thickness (11.5 µm) and stiffness (8.8 MPa) of the film actuators to match this range. The beating of the anisotropic artificial heart would cause periodic bending of the PDMS substrate, leading to the change of the resistance of an embedded strain sensor. Thus, the tissue mechanics of the heart-on-a-chip can be evaluated by recording the real-time resistance signal.

Going a step further, Zhao's team had developed a series of heart-on-a-chip systems based on visually perceptible optical signals rather than electrical ones, eliminating circuit connections and applying the devices in drug testing.[201–205] For example, they assembled cardiomyocytes on a hydrogel substrate with surface microgrooves (**Figure 11**a,b).[201] The 3D microstructures of the substrate surfaces induced the anisotropic assembly and synchronous beating of the cardiomyocytes. Meanwhile, the periodic porous inverse opal structure of the hydrogel substrate also imparted unique structural color to the heart-on-a-chip, which could shift with the beating of the tissues (Figure 11c). Thus, the contraction force of the cardiomyocytes was converted into easily detectable optical signals. Then different concentrations of isoproterenol were applied to the device, and accordingly, the cellular responses were investigated by measuring the reflection spectrum of the inverse opal film (Figure 11d,e). These results showcased the application value of SFAs-based organ-on-a-chip platforms in biosensing, drug screening, and related areas.

## 7. Conclusion and Perspective

SFA is a class of intelligent material with tunable 3D structures and stimuli-responsive transformation/motion abilities. Owing to their flexible nature, these polymer-based actuating systems are close to the mechanical properties of biological organisms and applicable to biological interfaces. Besides, they could dynamically change their physicochemical properties under external stimuli and achieve shape deformations as well

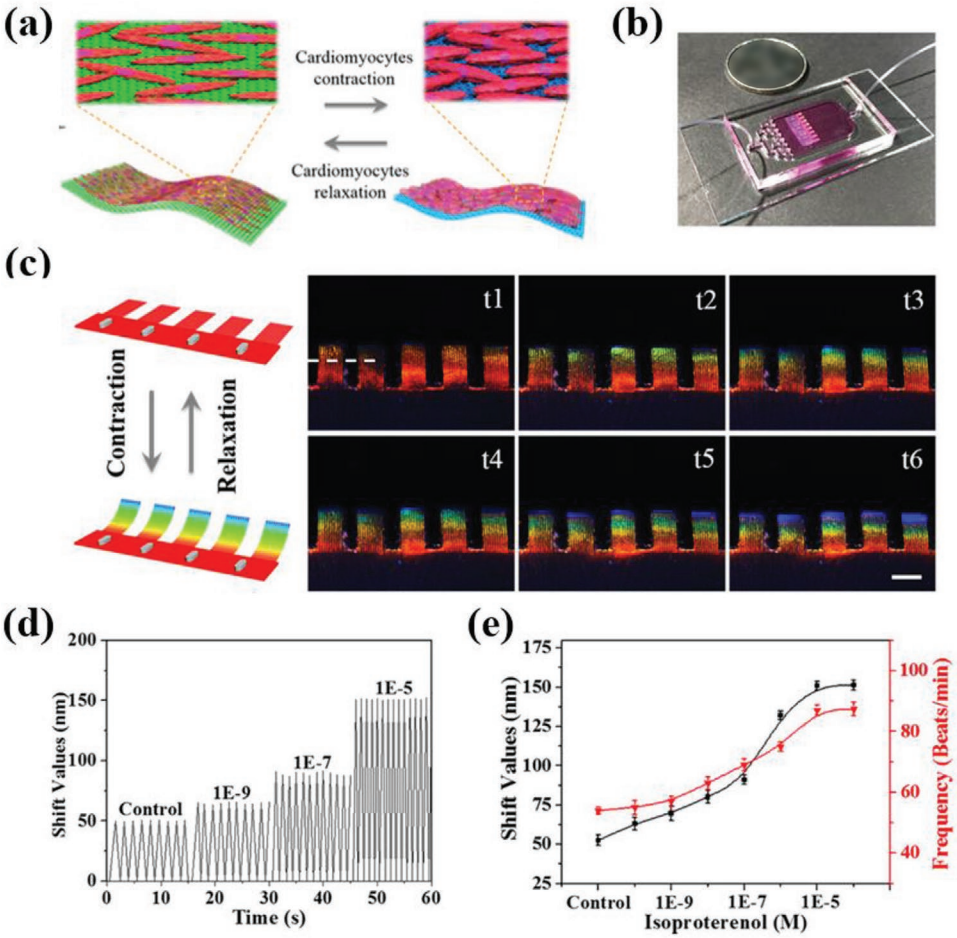


**Figure 11.** SFAs-based organ-on-a-chip system. Reproduced with permission.[201] Copyright 2018, American Association for the Advancement of Science. a) Schematic diagram of the actuating mechanism of the structural color heart-on-a-chip. b) Photograph image of the structural color heart-on-a-chip. c) Schematic diagram and optical microscopic image of the bend-up process of the actuator during one myocardial beating cycle. d) The time-variant shift values of the reflection peak of the structural color film when the cardiomyocytes were treated with different concentrations of isoproterenol. e) The average shift values of the reflection peak of the structural color film (left) and the beating frequency of the cardiomyocytes (right) as a function of isoproterenol concentration. Scale bar in (c) is 1 mm.

as mechanical locomotions. These properties have made them widely studied in the biomedical field. Here, we focused our view on SFAs for their biomedical applications. We first introduced the fabrication of SFAs, including direct casting, photolithography, 3D printing, electrospinning, and self-assembly. We then highlighted the topology design of SFAs, such as bilayer structure, oriented structure, patterned structure, and others. After this, we introduced the main composing materials of the SFAs and listed the actuating mechanisms under various stimuli including thermal, light, electric, pH, etc. Finally, we presented the applications of SFAs in the biomedical field, with emphasis on soft robotics, tissue engineering, delivery system, and organ-on-a-chip.

Despite that the last few decades have witnessed the rapid development of SFAs in the field of biomedical applications, there remains considerable room for the evolution of these materials in the following directions. First, it is necessary to improve the accuracy of the 3D deformations of SFAs under external stimuli, as well as the efficiency of performing complex movements in a way mimicking animal motion. The development of a comprehensive theoretical framework could serve as a guide for the design of the SFAs. As such, it is also important to combine advanced molecular design, chemical synthesis, and microfabrication technology to develop novel functional materials, and incorporate sophisticated structural design to construct flexible smart devices that can achieve precise 3D reconfiguration and high-efficient maneuverable locomotion. To achieve these goals, interdisciplinary collaborative efforts are required including mathematics, chemistry, material science, biology, and microelectromechanical processing. Second, the responsiveness feature of SFAs is often compromised by the biocompatibility of the materials. Also, the manufacturing process may be accompanied by environmental pollution due to the possible damaging intermediates. Therefore, the development of intelligent biomedical materials that are more environmentally friendly and compatible to human body is an important direction for the future research of SFAs. To this end, natural polymers, which are abundant in the mother nature and superior in their renewability and brilliant biocompatibility are expected to be exploited in the future. Third, multifunctional actuating systems that can work collaboratively under multiple external stimuli and perform more sophisticated instructions by integrating multiple responsive units are greatly anticipated. In summary, compared with the rapid, accurate and complex biological actuating systems in nature, artificial SFAs still have a long way to go. Nonetheless, there is no doubt that the convergence of functional polymer materials and shape-adaptive properties will continue standing at the forefront and stride forward toward practical biomedical applications in the future.

## Acknowledgements

This work was supported by the National Key Research and Development Program of China (2020YFB1313100), the National Natural Science Foundation of China (22002018), the Innovative Research Team of High-level Local University in Shanghai, and the Professor of Special Appointment (Eastern Scholar) at Shanghai Institutions of Higher Learning (SSH1340011).

## Conflict of Interest

The authors declare no conflict of interest.

## Keywords

biomedical applications, film actuators, responsive polymers, soft robotics

Received: August 25, 2021
Revised: November 23, 2021
Published online: January 17, 2022

[1] E. Acome, S. K. Mitchell, T. G. Morrissey, M. B. Emmett, C. Benjamin, M. King, M. Radakovitz, C. Keplinger, *Science* **2018**, *359*, 61.
[2] L. Hines, K. Petersen, G. Z. Lum, M. Sitti, *Adv. Mater.* **2017**, *29*, 1603483.
[3] Y. S. Kim, M. Liu, Y. Ishida, Y. Ebina, M. Osada, T. Sasaki, T. Hikima, M. Takata, T. Aida, *Nat. Mater.* **2015**, *14*, 1002.
[4] A. Rafsanjani, Y. Zhang, B. Liu, S. M. Rubinstein, K. Bertoldi, *Sci. Rob.* **2018**, *3*, eaar7555.
[5] A. Miriyev, K. Stack, H. Lipson, *Nat. Commun.* **2017**, *8*, 596.
[6] M. Schaffner, J. A. Faber, L. Pianegonda, P. A. Ruhs, F. Coulter, A. R. Studart, *Nat. Commun.* **2018**, *9*, 878.
[7] J. Shintake, S. Rosset, B. Schubert, D. Floreano, H. Shea, *Adv. Mater.* **2016**, *28*, 231.
[8] G. M. Whitesides, *Angew. Chem., Int. Ed.* **2018**, *57*, 4258.
[9] D. Rus, M. T. Tolley, *Nature* **2015**, *521*, 467.
[10] S. Kim, C. Laschi, B. Trimmer, *Trends Biotechnol.* **2013**, *31*, 287.
[11] D. Trivedi, C. D. Rahn, W. M. Kier, I. D. Walker, *Appl. Bionics Biomech.* **2008**, *5*, 99.
[12] A. G. Volkov, J. C. Foster, K. D. Baker, V. S. Markin, *Plant Signaling Behav.* **2010**, *5*, 1211.
[13] J. Dumais, Y. Forterre, *Annu. Rev. Fluid Mech.* **2012**, *44*, 453.
[14] S. M. Mirvakili, I. W. Hunter, *Adv. Mater.* **2018**, *30*, 1704407.
[15] J. Shang, X. Le, J. Zhang, T. Chen, P. Theato, *Polym. Chem.* **2019**, *10*, 1036.
[16] C. Ma, W. Lu, X. Yang, J. He, X. Le, L. Wang, J. Zhang, M. J. Serpe, Y. Huang, T. Chen, *Adv. Funct. Mater.* **2018**, *28*, 1704568.
[17] J. M. McCracken, B. R. Donovan, T. J. White, *Adv. Mater.* **2020**, *32*, 1906564.
[18] L. Ionov, *Mater. Today* **2014**, *17*, 494.
[19] M. Lopez-Valdeolivas, D. Liu, D. J. Broer, C. Sanchez-Somolinos, *Macromol. Rapid Commun.* **2018**, *39*, 1700710.
[20] M. Ma, L. Guo, D. G. Anderson, R. Langer, *Science* **2013**, *339*, 186.
[21] M. Wei, Y. Gao, X. Li, M. J. Serpe, *Polym. Chem.* **2017**, *8*, 127.
[22] Q. Zhao, J. W. C. Dunlop, X. Qiu, F. Huang, Z. Zhang, J. Heyda, J. Dzubiella, M. Antonietti, J. Yuan, *Nat. Commun.* **2014**, *5*, 4293.
[23] M. Cianchetti, C. Laschi, A. Menciassi, P. Dario, *Nat. Rev. Mater.* **2018**, *3*, 143.
[24] L. Ionov, *Adv. Funct. Mater.* **2013**, *23*, 4555.
[25] W. A. D. M. Jayathilaka, K. Qi, Y. Qin, A. Chinnappan, W. Serrano-Garcia, C. Baskar, H. Wang, J. He, S. Cui, S. W. Thomas, S. Ramakrishna, *Adv. Mater.* **2019**, *31*, 1805921.
[26] J. M. Korde, B. Kandasubramanian, *Chem. Eng. J.* **2020**, *379*, 122430.
[27] S. I. Rich, R. J. Wood, C. Majidi, *Nat. Electron.* **2018**, *1*, 102.
[28] C. Zhang, B. Wu, Y. Zhou, F. Zhou, W. Liu, Z. Wang, *Chem. Soc. Rev.* **2020**, *49*, 3605.
[29] X. Le, W. Lu, J. Zhang, T. Chen, *Adv. Sci.* **2019**, *6*, 1801584.
[30] K. Sano, Y. Ishida, T. Aida, *Angew. Chem., Int. Ed.* **2018**, *57*, 2532.

[31] Q. Wang, L. Yu, M. Yu, D. Zhao, P. Song, H. Chi, L. Guo, H. Yang, *Macromol. Rapid Commun.* **2017**, *38*, 1600699.
[32] J. P. F. Lagerwall, G. Scalia, *Curr. Appl. Phys.* **2012**, *12*, 1387.
[33] H. Qin, T. Zhang, N. Li, H.-P. Cong, S.-H. Yu, *Nat. Commun.* **2019**, *10*, 2202.
[34] R. V. Martinez, C. R. Fish, X. Chen, G. M. Whitesides, *Adv. Funct. Mater.* **2012**, *22*, 1376.
[35] B. Mosadegh, P. Polygerinos, C. Keplinger, S. Wennstedt, R. F. Shepherd, U. Gupta, J. Shim, K. Bertoldi, C. J. Walsh, G. M. Whitesides, *Adv. Funct. Mater.* **2014**, *24*, 2163.
[36] A. D. Mazzeo, M. E. Lustrino, D. E. Hardt, *Polym. Eng. Sci.* **2012**, *52*, 80.
[37] D.-Y. Zhao, Z.-P. Huang, M.-J. Wang, T. Wang, Y. Jin, *J. Mater. Process. Technol.* **2012**, *212*, 198.
[38] R. K. Katzschmann, A. D. Marchese, D. Rus, *Soft Rob.* **2015**, *2*, 155.
[39] A. D. Marchese, C. D. Onal, D. Rus, *Soft Rob.* **2014**, *1*, 75.
[40] J. Kim, J. A. Hanna, M. Byun, C. D. Santangelo, R. C. Hayward, *Science* **2012**, *335*, 1201.
[41] T. J. Kim, Y. H. Jung, H. L. Zhang, K. Kim, J. Lee, Z. Q. Ma, *ACS Appl. Mater. Interfaces* **2018**, *10*, 8117.
[42] R. Guo, L. Sheng, H. Y. Gong, J. Liu, *Sci. China: Technol. Sci.* **2018**, *61*, 516.
[43] Y. Ji, Y. Xing, X. Li, L.-H. Shao, *Nanomaterials* **2019**, *9*, 1704.
[44] L. Ceamanos, Z. Kahveci, M. López-Valdeolivas, D. Liu, D. J. Broer, C. Sánchez-Somolinos, *ACS Appl. Mater. Interfaces* **2020**, *12*, 44195.
[45] S. Vanaei, M. S. Parizi, S. Vanaei, F. Salemizadehparizi, H. R. Vanaei, *Eng. Regen.* **2021**, *2*, 1.
[46] C. G. Harris, N. J. S. Jursik, W. E. Rochefort, T. W. Walker, *Front. Mech. Eng.* **2019**, *5*, 37.
[47] F. Liravi, E. Toyserkani, *Addit. Manuf.* **2018**, *24*, 232.
[48] J. M. Unagolla, A. C. Jayasuriya, *Appl. Mater. Today* **2020**, *18*, 100479.
[49] H. Yuk, B. Lu, S. Lin, K. Qu, J. Xu, J. Luo, X. Zhao, *Nat. Commun.* **2020**, *11*, 1604.
[50] E. Sachyani Keneth, A. Kamyshny, M. Totaro, L. Beccai, S. Magdassi, *Adv. Mater.* **2021**, *33*, 2003387.
[51] G. Stano, L. Arleo, G. Percoco, *Micromachines* **2020**, *11*, 485.
[52] Z. Wang, Y. Wang, Z. Wang, Q. He, C. Li, S. Cai, *ACS Appl. Mater. Interfaces* **2021**, *13*, 24164.
[53] A. Zolfagharian, M. Denk, M. Bodaghi, A. Z. Kouzani, A. Kaynak, *Acta Mech. Solida Sin.* **2020**, *33*, 418.
[54] M. Babaei, S. Kim, C. Velez, D. K. Patel, S. Bergbreiter, *J. Microelectromech. Syst.* **2020**, *29*, 797.
[55] K. Thetpraphi, W. Kanlayakan, S. Chaipo, G. Moretto, J. Kuhn, D. Audigier, L. Minh Quyen, P.-J. Cottinet, L. Petit, J.-F. Capsal, *Addit. Manuf.* **2021**, *47*, 102199.
[56] Y. Wang, Y. Zhou, W. Li, Z. Liu, B. Zhou, S. Wen, L. Jiang, S. Chen, J. Ma, A. Betts, S. Jerrams, F. Zhou, *Smart Mater. Struct.* **2021**, *30*, 025001.
[57] E. Axpe, M. L. Oyen, *Int. J. Mol. Sci.* **2016**, *17*, 1976.
[58] F. Guillemot, B. Guillotin, A. Fontaine, M. Ali, S. Catros, V. Keriquel, J.-C. Fricain, M. Remy, R. Bareille, J. Amedee-Vilamitjana, *MRS Bull.* **2011**, *36*, 1015.
[59] W. E. KingIII, G. L. Bowlin, *Polymers* **2021**, *13*, 1097.
[60] Y. Zhao, J. Sheng, D. Xu, M. Gao, Q. Meng, D. Wu, L. Wang, W. Lv, Q. Chen, J. Xiao, D. Sun, *Polymers* **2018**, *10*, 803.
[61] J. M. Deitzel, J. D. Kleinmeyer, J. K. Hirvonen, N. C. B. Tan, *Polymer* **2001**, *42*, 8163.
[62] M.-H. Jung, Y. J. Yun, M.-J. Chu, M. G. Kang, *Chem. - Eur. J.* **2013**, *19*, 8543.
[63] A. R. Tan, J. L. Ifkovits, B. M. Baker, D. M. Brey, R. L. Mauck, J. A. Burdick, *J. Biomed. Mater. Res., Part A* **2008**, *87A*, 1034.
[64] C. Cui, S. Sun, S. Wu, S. Chen, J. Ma, F. Zhou, *Eng. Regen.* **2021**, *2*, 82.
[65] G. Y. Yun, H. S. Kim, J. Kim, K. Kim, C. Yang, *Sens. Actuators, A* **2008**, *141*, 530.
[66] K. Miyakawa, Y. Takahama, K. Kida, K. Sato, M. Kushida, *Jpn. J. Appl. Phys.* **2020**, *59*, SIIF02.
[67] Z.-M. Huang, Y. Z. Zhang, M. Kotaki, S. Ramakrishna, *Compos. Sci. Technol.* **2003**, *63*, 2223.
[68] J. J. Sun, X. X. Ji, G. H. Li, Y. Zhang, N. Liu, H. G. Li, M. H. Qin, Z. W. Yuan, *J. Mater. Chem. C* **2019**, *7*, 104.
[69] Z. Zhang, Z. Chen, Y. Wang, J. Chi, Y. Wang, Y. Zhao, *Small Methods* **2019**, *3*, 1900519.
[70] C.-T. Chen, R.-C. Peng, *Smart Mater. Struct.* **2021**, *30*, 075010.
[71] G. Ehrmann, A. Ehrmann, *J. Appl. Polym. Sci.* **2021**, *138*, 50847.
[72] J. Li, C. Wu, P. K. Chu, M. Gelinsky, *Mater. Sci. Eng., R* **2020**, *140*, 100543.
[73] J. C. Kade, P. D. Dalton, *Adv. Healthcare Mater.* **2021**, *10*, 2001232.
[74] P. D. Dalton, T. B. F. Woodfield, V. Mironov, J. Groll, *Adv. Sci.* **2020**, *7*, 1902953.
[75] M. Santschi, A. Vernengo, D. Eglin, M. D'Este, K. Wuertz-Kozak, *Curr. Opin. Biomed. Eng.* **2019**, *10*, 116.
[76] D. Morales, E. Palleau, M. D. Dickey, O. D. Velev, *Soft Matter* **2014**, *10*, 1337.
[77] H. L. Lim, J. C. Chuang, T. Tran, A. Aung, G. Arya, S. Varghese, *Adv. Funct. Mater.* **2011**, *21*, 55.
[78] L. Wang, Y. Liu, Y. Cheng, X. G. Cui, H. Q. Lian, Y. R. Liang, F. Chen, H. Wang, W. L. Guo, H. Q. Li, M. F. Zhu, H. Ihara, *Adv. Sci.* **2015**, *2*, 6.
[79] X. Zhang, L. S. Chen, C. Zhang, L. Q. Liao, *ACS Appl. Mater. Interfaces* **2021**, *13*, 18175.
[80] C. Y. Huang, T. R. Ger, M. F. Lai, W. Y. Chen, H. T. Huang, J. Y. Chen, P. J. Wang, Z. H. Wei, *J. Appl. Phys.* **2015**, *117*, 4.
[81] J. Zheng, P. Xiao, X. Le, W. Lu, P. Théato, C. Ma, B. Du, J. Zhang, Y. Huang, T. Chen, *J. Mater. Chem. C* **2018**, *6*, 1320.
[82] X. Lu, H. Zhang, G. Fei, B. Yu, X. Tong, H. Xia, Y. Zhao, *Adv. Mater.* **2018**, *30*, 1706597.
[83] A. Sydney Gladman, E. A. Matsumoto, R. G. Nuzzo, L. Mahadevan, J. A. Lewis, *Nat. Mater.* **2016**, *15*, 413.
[84] Z. L. Wu, M. Moshe, J. Greener, H. Therien-Aubin, Z. Nie, E. Sharon, E. Kumacheva, *Nat. Commun.* **2013**, *4*, 1586.
[85] X. Wang, H. Huang, H. Liu, F. Rehfeldt, X. Wang, K. Zhang, *Macromol. Chem. Phys.* **2019**, *220*, 1800562.
[86] R. C. Luo, J. Wu, N. D. Dinh, C. H. Chen, *Adv. Funct. Mater.* **2015**, *25*, 7272.
[87] X. X. Le, Y. C. Zhang, W. Lu, L. Wang, J. Zheng, I. Ali, J. W. Zhang, Y. J. Huang, M. J. Serpe, X. T. Yang, X. D. Fan, T. Chen, *Macromol. Rapid Commun.* **2018**, *39*, 1800019.
[88] R. Luo, J. Wu, N.-D. Dinh, C.-H. Chen, *Adv. Funct. Mater.* **2015**, *25*, 7272.
[89] Y. Tan, D. Wang, H. Xu, Y. Yang, W. An, L. Yu, Z. Xiao, S. Xu, *Macromol. Rapid Commun.* **2018**, *39*, 1700863.
[90] C. Ma, T. Li, Q. Zhao, X. Yang, J. Wu, Y. Luo, T. Xie, *Adv. Mater.* **2014**, *26*, 5665.
[91] C. Yao, Z. Liu, C. Yang, W. Wang, X.-J. Ju, R. Xie, L.-Y. Chu, *ACS Appl. Mater. Interfaces* **2016**, *8*, 21721.
[92] L. Vannozzi, I. C. Yasa, H. Ceylan, A. Menciassi, L. Ricotti, M. Sitti, *Macromol. Biosci.* **2018**, *18*, 1700377.
[93] E. Käpylä, S. M. Delgado, A. M. Kasko, *ACS Appl. Mater. Interfaces* **2016**, *8*, 17885.
[94] Y. Piao, H. You, T. Xu, H.-P. Bei, I. Z. Piwko, Y. Y. Kwan, X. Zhao, *Eng. Regen.* **2021**, *2*, 47.
[95] M. Safonov, J. You, J. Lee, V. L. Safonov, D. Berman, D. Zhu, *Eng. Regen.* **2020**, *1*, 1.
[96] T. Malachowski, A. Hassel, *Eng. Regen.* **2020**, *1*, 35.
[97] A. Lendlein, S. Kelch, *Angew. Chem., Int. Ed.* **2002**, *41*, 2034.
[98] B. Q. Y. Chan, Z. W. K. Low, S. J. W. Heng, S. Y. Chan, C. Owh, X. J. Loh, *ACS Appl. Mater. Interfaces* **2016**, *8*, 10070.
[99] P.-G. De Gennes, M. Hébert, R. Kant, *Macromol. Symp.* **1997**, *113*, 39.
[100] T. J. White, D. J. Broer, *Nat. Mater.* **2015**, *14*, 1087.
[101] T. J. White, *J. Polym. Sci., Part B: Polym. Phys.* **2018**, *56*, 695.

[102] L. T. de Haan, V. Gimenez-Pinto, A. Konya, T.-S. Nguyen, J. M. N. Verjans, C. Sánchez-Somolinos, J. V. Selinger, R. L. B. Selinger, D. J. Broer, A. P. H. J. Schenning, *Adv. Funct. Mater.* **2014**, *24*, 1251.
[103] H. Meng, J. L. Hu, *J. Intell. Mater. Syst. Struct.* **2010**, *21*, 859.
[104] L. Hu, Q. Zhang, X. Li, M. J. Serpe, *Mater. Horiz.* **2019**, *6*, 1774.
[105] F. Liu, M. W. Urban, *Prog. Polym. Sci.* **2010**, *35*, 3.
[106] H. G. Schild, *Prog. Polym. Sci.* **1992**, *17*, 163.
[107] M. Amjadi, M. Sitti, *Adv. Sci.* **2018**, *5*, 1800239.
[108] L. Chen, M. Weng, P. Zhou, F. Huang, C. Liu, S. Fan, W. Zhang, *Adv. Funct. Mater.* **2019**, *29*, 1806057.
[109] W. J. Zheng, N. An, J. H. Yang, J. Zhou, Y. M. Chen, *ACS Appl. Mater. Interfaces* **2015**, *7*, 1758.
[110] X. Xiao, H. Ma, X. Zhang, *ACS Nano* **2021**, *15*, 12826.
[111] Y. Hu, J. Liu, L. Chang, L. Yang, A. Xu, K. Qi, P. Lu, G. Wu, W. Chen, Y. Wu, *Adv. Funct. Mater.* **2017**, *27*, 1704388.
[112] P. Zhou, L. Chen, L. Yao, M. Weng, W. Zhang, *Nanoscale* **2018**, *10*, 8422.
[113] B. Han, Y.-L. Zhang, L. Zhu, Y. Li, Z.-C. Ma, Y.-Q. Liu, X.-L. Zhang, X.-W. Cao, Q.-D. Chen, C.-W. Qiu, H.-B. Sun, *Adv. Mater.* **2019**, *31*, 1806386.
[114] W. Sang, L. Zhao, R. Tang, Y. Wu, C. Zhu, J. Liu, *Macromol. Mater. Eng.* **2017**, *302*, 1700239.
[115] S. Klumpp, B. Kiani, P. Vach, D. Faivre, *Phys. Scr.* **2015**, *T165*, 014044.
[116] K. Bente, A. Codutti, F. Bachmann, D. Faivre, *Small* **2018**, *14*, 1704374.
[117] M. M. Stanton, B.-W. Park, A. Miguel-López, X. Ma, M. Sitti, S. Sánchez, *Small* **2017**, *13*, 1603679.
[118] C. R. Mayer, V. Cabuil, T. Lalot, R. Thouvenot, *Adv. Mater.* **2000**, *12*, 417.
[119] S. Brule, M. Levy, C. Wilhelm, D. Letourneur, F. Gazeau, C. Menager, C. Le Visage, *Adv. Mater.* **2011**, *23*, 787.
[120] J. I. Kim, C. Chun, B. Kim, J. M. Hong, J. K. Cho, S. H. Lee, S. C. Song, *Biomaterials* **2012**, *33*, 218.
[121] N. S. Satarkar, W. L. Zhang, R. E. Eitel, J. Z. Hilt, *Lab Chip* **2009**, *9*, 1773.
[122] Y. Wang, Q. Guo, G. Su, J. Cao, J. Liu, X. Zhang, *Adv. Funct. Mater.* **2019**, *29*, 1906198.
[123] R. Baumgartner, A. Kogler, J. M. Stadlbauer, C. C. Foo, R. Kaltseis, M. Baumgartner, G. Mao, C. Keplinger, S. J. A. Koh, N. Arnold, Z. Suo, M. Kaltenbrunner, S. Bauer, *Adv. Sci.* **2020**, *7*, 1903391.
[124] D. Chen, Q. Liu, Z. Han, J. Zhang, H. Song, K. Wang, Z. Song, S. Wen, Y. Zhou, C. Yan, Y. Shi, *Adv. Sci.* **2020**, *7*, 2000584.
[125] Y. Wang, X. Huang, X. Zhang, *Nat. Commun.* **2021**, *12*, 1291.
[126] J. S. Scarpa, D. D. Mueller, I. M. Klotz, *J. Am. Chem. Soc.* **1967**, *89*, 6024.
[127] Y. Cheng, C. Huang, D. Yang, K. Ren, J. Wei, *J. Mater. Chem. B* **2018**, *6*, 8170.
[128] Y. Liu, L. Xing, Q. Zhang, Q. Mu, P. Liu, K. Chen, L. Chen, X. Zhang, K. Wang, Y. Wei, *Colloid Polym. Sci.* **2016**, *294*, 617.
[129] X. Peng, H. Wang, *J. Polym. Sci., Part B: Polym. Phys.* **2018**, *56*, 1314.
[130] S. Xiao, M. Zhang, X. He, L. Huang, Y. Zhang, B. Ren, M. Zhong, Y. Chang, J. Yang, J. Zheng, *ACS Appl. Mater. Interfaces* **2018**, *10*, 21642.
[131] L. Liu, A. Ghaemi, S. Gekle, S. Agarwal, *Adv. Mater.* **2016**, *28*, 9792.
[132] B. Jin, H. Song, R. Jiang, J. Song, Q. Zhao, T. Xie, *Sci. Adv.* **2018**, *4*, eaao3865.
[133] G. J. Berg, M. K. McBride, C. Wang, C. N. Bowman, *Polymer* **2014**, *55*, 5849.
[134] F. D. Jochum, P. Theato, *Chem. Soc. Rev.* **2013**, *42*, 7468.
[135] D.-D. Han, Y.-L. Zhang, J.-N. Ma, Y.-Q. Liu, B. Han, H.-B. Sun, *Adv. Mater.* **2016**, *28*, 8328.
[136] J. Shang, S. Lin, P. Theato, *Polym. Chem.* **2018**, *9*, 3232.
[137] Z.-B. Wen, D. Liu, X.-Y. Li, C.-H. Zhu, R.-F. Shao, R. Visvanathan, N. A. Clark, K.-K. Yang, Y.-Z. Wang, *ACS Appl. Mater. Interfaces* **2017**, *9*, 24947.
[138] S. Wu, H.-J. Butt, *Adv. Mater.* **2016**, *28*, 1208.
[139] A. M. Marconnet, M. A. Panzer, K. E. Goodson, *Rev. Mod. Phys.* **2013**, *85*, 1295.
[140] X. Huang, Q. Qian, X. Zhang, W. Du, H. Xu, Y. Wang, *Part. Part. Syst. Charact.* **2013**, *30*, 235.
[141] M.-F. Yu, B. S. Files, S. Arepalli, R. S. Ruoff, *Phys. Rev. Lett.* **2000**, *84*, 5552.
[142] D. Hua, X. Zhang, Z. Ji, C. Yan, B. Yu, Y. Li, X. Wang, F. Zhou, *J. Mater. Chem. C* **2018**, *6*, 2123.
[143] J. Deng, J. Li, P. Chen, X. Fang, X. Sun, Y. Jiang, W. Weng, B. Wang, H. Peng, *J. Am. Chem. Soc.* **2016**, *138*, 225.
[144] B. Han, Y.-L. Zhang, Q.-D. Chen, H.-B. Sun, *Adv. Funct. Mater.* **2018**, *28*, 1802235.
[145] M. Naguib, M. Kurtoglu, V. Presser, J. Lu, J. Niu, M. Heon, L. Hultman, Y. Gogotsi, M. W. Barsoum, *Adv. Mater.* **2011**, *23*, 4248.
[146] F. Zhao, Y. Zhao, N. Chen, L. Qu, *Mater. Today* **2016**, *19*, 146.
[147] K. S. Novoselov, V. I. Fal'ko, L. Colombo, P. R. Gellert, M. G. Schwab, K. Kim, *Nature* **2012**, *490*, 192.
[148] D. Niu, W. Jiang, H. Liu, T. Zhao, B. Lei, Y. Li, L. Yin, Y. Shi, B. Chen, B. Lu, *Sci. Rep.* **2016**, *6*, 27366.
[149] J.-N. Wang, Y.-L. Zhang, Y. Liu, W. Zheng, L. P. Lee, H.-B. Sun, *Nanoscale* **2015**, *7*, 7101.
[150] Y. Jiang, C. Hu, H. Cheng, C. Li, T. Xu, Y. Zhao, H. Shao, L. Qu, *ACS Nano* **2016**, *10*, 4735.
[151] W. Jiang, D. Niu, H. Liu, C. Wang, T. Zhao, L. Yin, Y. Shi, B. Chen, Y. Ding, B. Lu, *Adv. Funct. Mater.* **2014**, *24*, 7598.
[152] G. Fugallo, A. Cepellotti, L. Paulatto, M. Lazzeri, N. Marzari, F. Mauri, *Nano Lett.* **2014**, *14*, 6109.
[153] K. Hantanasirisakul, Y. Gogotsi, *Adv. Mater.* **2018**, *30*, 1804779.
[154] X.-H. Zha, J. Zhou, Y. Zhou, Q. Huang, J. He, J. S. Francisco, K. Luo, S. Du, *Nanoscale* **2016**, *8*, 6110.
[155] R. Li, L. Zhang, L. Shi, P. Wang, *ACS Nano* **2017**, *11*, 3752.
[156] G. Cai, J.-H. Ciou, Y. Liu, Y. Jiang, P. S. Lee, *Sci. Adv.* **2019**, *5*, eaaw7956.
[157] H. S. Wang, J. Cho, D. S. Song, J. H. Jang, J. Y. Jho, J. H. Park, *ACS Appl. Mater. Interfaces* **2017**, *9*, 21998.
[158] T. Wang, M. Farajollahi, Y. S. Choi, I.-T. Lin, J. E. Marshall, N. M. Thompson, S. Kar-Narayan, J. D. W. Madden, S. K. Smoukov, *Interface Focus* **2016**, *6*, 20160026.
[159] S. Shian, K. Bertoldi, D. R. Clarke, *Adv. Mater.* **2015**, *27*, 6814.
[160] A. Ahiabu, M. J. Serpe, *ACS Omega* **2017**, *2*, 1769.
[161] G. Vancoillie, R. Hoogenboom, *Polym. Chem.* **2016**, *7*, 5484.
[162] J. Xu, D. Yang, R. Lv, B. Liu, S. Gai, F. He, C. Li, P. Yang, *J. Mater. Chem. B* **2016**, *4*, 5883.
[163] K. Kim, W. C. W. Chen, Y. Heo, Y. Wang, *Prog. Polym. Sci.* **2016**, *60*, 18.
[164] E. B. Bahadır, M. K. Sezgintürk, *Talanta* **2016**, *148*, 427.
[165] Z. Han, P. Wang, G. Mao, T. Yin, D. Zhong, B. Yiming, X. Hu, Z. Jia, G. Nian, S. Qu, W. Yang, *ACS Appl. Mater. Interfaces* **2020**, *12*, 12010.
[166] H. Li, G. Go, S. Y. Ko, J.-O. Park, S. Park, *Smart Mater. Struct.* **2016**, *25*, 027001.
[167] L. Zhang, S. Chizhik, Y. Wen, P. Naumov, *Adv. Funct. Mater.* **2016**, *26*, 1040.
[168] Y. He, K. Kong, Z. Guo, W. Fang, Z. Ma, H. Pan, R. Tang, Z. Liu, *Adv. Funct. Mater.* **2021**, *31*, 2101291.
[169] N. Osada, H. Takeda, A. Furukawa, M. Awang, *J. Trop. Ecol.* **2002**, *18*, 309.
[170] J. R. Hagler, B. N. Peterson, A. R. Murphy, J. M. Leger, *J. Appl. Polym. Sci.* **2019**, *136*, 46922.
[171] P. Mi, X.-J. Ju, R. Xie, H.-G. Wu, J. Ma, L.-Y. Chu, *Polymer* **2010**, *51*, 1648.
[172] Y. Shin, M. Y. Choi, J. Choi, J. H. Na, S. Y. Kim, *ACS Appl. Mater. Interfaces* **2021**, *13*, 15633.
[173] L. Yang, T. Zhang, W. Sun, *J. Appl. Polym. Sci.* **2020**, *137*, 49375.
[174] H. L. Guo, W. T. Dai, Y. Miao, Y. Z. Wang, D. Ma, W. Xue, *Chem. Eng. J.* **2018**, *339*, 459.

[175] L. Sun, Y. Yu, Z. Chen, F. Bian, F. Ye, L. Sun, Y. Zhao, *Chem. Soc. Rev.* **2020**, *49*, 4043.
[176] Z. Y. Mao, K. K. Zhu, L. L. Pan, G. Liu, T. Tang, Y. H. He, J. P. Huang, J. L. Hu, K. Chan, J. Lu, *Adv. Mater. Technol.* **2020**, *5*, 1900974.
[177] Y. Z. Wang, Z. J. Cheng, Z. G. Liu, H. J. Kang, Y. Y. Liu, *J. Mater. Chem. B* **2018**, *6*, 1668.
[178] G. Gerboni, M. Brancadoro, G. Tortora, A. Diodato, M. Cianchetti, A. Menciassi, *Smart Mater. Struct.* **2016**, *25*, 105025.
[179] S. Kim, C. Laschi, B. Trimmer, *Trends Biotechnol.* **2013**, *31*, 287.
[180] S. Huang, Y. Liu, Y. Zhao, Z. Ren, C. F. Guo, *Adv. Funct. Mater.* **2019**, *29*, 1805924.
[181] G.-Z. Yang, J. Bellingham, P. E. Dupont, P. Fischer, L. Floridi, R. Full, N. Jacobstein, V. Kumar, M. McNutt, R. Merrifield, B. J. Nelson, B. Scassellati, M. Taddeo, R. Taylor, M. Veloso, Z. L. Wang, R. Wood, *Sci. Rob.* **2018**, *3*, eaar7650.
[182] J. C. Breger, C. Yoon, R. Xiao, H. R. Kwag, M. O. Wang, J. P. Fisher, T. D. Nguyen, D. H. Gracias, *ACS Appl. Mater. Interfaces* **2015**, *7*, 3398.
[183] N. Bassik, A. Brafman, A. M. Zarafshar, M. Jamal, D. Luvsanjav, F. M. Selaru, D. H. Gracias, *J. Am. Chem. Soc.* **2010**, *132*, 16314.
[184] Q. Jin, Y. Yang, J. A. Jackson, C. Yoon, D. H. Gracias, *Nano Lett.* **2020**, *20*, 5383.
[185] E. Gultepe, J. S. Randhawa, S. Kadam, S. Yamanaka, F. M. Selaru, E. J. Shin, A. N. Kalloo, D. H. Gracias, *Adv. Mater.* **2013**, *25*, 514.
[186] A. Ghosh, Y. Liu, D. Artemov, D. H. Gracias, *Adv. Healthcare Mater.* **2021**, *10*, 2000869.
[187] S. Fusco, M. S. Sakar, S. Kennedy, C. Peters, R. Bottani, F. Starsich, A. Mao, G. A. Sotiriou, S. Pané, S. E. Pratsinis, D. Mooney, B. J. Nelson, *Adv. Mater.* **2014**, *26*, 952.
[188] K. Malachowski, M. Jamal, Q. Jin, B. Polat, C. J. Morris, D. H. Gracias, *Nano Lett.* **2014**, *14*, 4164.
[189] Q. L. Zhao, J. Wang, H. Q. Cui, H. X. Chen, Y. L. Wang, X. M. Du, *Adv. Funct. Mater.* **2018**, *28*, 1801027.
[190] J. Wang, H. Xiong, T. Zhu, Y. Liu, H. Pan, C. Fan, X. Zhao, W. W. Lu, *ACS Nano* **2020**, *14*, 12579.
[191] G. Stoychev, N. Puretskiy, L. Ionov, *Soft Matter* **2011**, *7*, 3277.
[192] N. Bassik, B. T. Abebe, K. E. Laflin, D. H. Gracias, *Polymer* **2010**, *51*, 6093.
[193] K. Malachowski, J. Breger, H. R. Kwag, M. O. Wang, J. P. Fisher, F. M. Selaru, D. H. Gracias, *Angew. Chem., Int. Ed.* **2014**, *53*, 8045.
[194] K. Kobayashi, C. Yoon, S. H. Oh, J. V. Pagaduan, D. H. Gracias, *ACS Appl. Mater. Interfaces* **2019**, *11*, 151.
[195] L. Shang, C. Shao, J. Chi, Y. Zhao, *Acc. Mater. Res.* **2021**, *2*, 59.
[196] Z. Q. Luo, D. E. Weiss, Q. Y. Liu, B. Z. Tian, *Nano Res.* **2018**, *11*, 3009.
[197] L. Shang, W. Zhang, K. Xu, Y. Zhao, *Mater. Horiz.* **2019**, *6*, 945.
[198] F. Zheng, F. Fu, Y. Cheng, C. Wang, Y. Zhao, Z. Gu, *Small* **2016**, *12*, 2253.
[199] J. U. Lind, T. A. Busbee, A. D. Valentine, F. S. Pasqualini, H. Yuan, M. Yadid, S.-J. Park, A. Kotikian, A. P. Nesmith, P. H. Campbell, J. J. Vlassak, J. A. Lewis, K. K. Parker, *Nat. Mater.* **2017**, *16*, 303.
[200] G. Wang, M. L. McCain, L. Yang, A. He, F. S. Pasqualini, A. Agarwal, H. Yuan, D. Jiang, D. Zhang, L. Zangi, J. Geva, A. E. Roberts, Q. Ma, J. Ding, J. Chen, D.-Z. Wang, K. Li, J. Wang, R. J. A. Wanders, W. Kulik, F. M. Vaz, M. A. Laflamme, C. E. Murry, K. R. Chien, R. I. Kelley, G. M. Church, K. K. Parker, W. T. Pu, *Nat. Med.* **2014**, *20*, 616.
[201] F. Fu, L. Shang, Z. Chen, Y. Yu, Y. Zhao, *Sci. Rob.* **2018**, *3*, eaar8580.
[202] L. Sun, Z. Chen, F. Bian, Y. Zhao, *Adv. Funct. Mater.* **2020**, *30*, 1907820.
[203] Z. Chen, F. Fu, Y. Yu, H. Wang, Y. Shang, Y. Zhao, *Adv. Mater.* **2019**, *31*, 1805431.
[204] L. Li, Z. Chen, C. Shao, L. Sun, L. Sun, Y. Zhao, *Adv. Funct. Mater.* **2020**, *30*, 1906353.
[205] Y. Shang, Z. Chen, F. Fu, L. Sun, C. Shao, W. Jin, H. Liu, Y. Zhao, *ACS Nano* **2019**, *13*, 796.

**Zhuohao Zhang** is currently a Ph.D. candidate at Fudan University. He received his Bachelor's degree and Master's degree in Biomedical Engineering at Southeast University in 2019 and 2021. He started his Ph.D. in the Institutes of Biomedical Sciences at Fudan University in 2021. His current scientific interests include functional polymers and their biomedical applications.

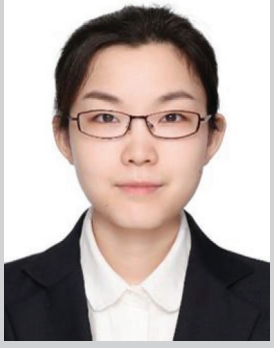

**Luoran Shang** is currently an assistant professor at the Institutes of Biomedical Sciences, Fudan University. She received her Ph.D. degree from Southeast University in 2017 under the supervision of Prof. Yuanjin Zhao. She worked as a postdoctoral fellow at Harvard University with Prof. David Weitz from 2017 to 2019. Her current scientific interests are focused on microfluidic fabrication of structural color materials.